

## Manuscript # acp-2021-328

### Responses to Referee #1

Ren et al. assess the contributions from local emissions and transport to PM<sub>2.5</sub> concentrations in Chinese regions during three periods when COVID-19 affected the socioeconomic activity of the country at the beginning of 2020. In principle, the topic is interesting and relevant, but I have major reservations concerning the chosen methods and the documentation thereof as well as the interpretation and discussion of the results.

We thank the editor for all the insightful comments. Below, please see our point-by-point response (in blue) to the specific comments and suggestions and the changes that have been made to the manuscript, in effort to take into account all the comments raised here.

The finding of regionally increasing PM<sub>2.5</sub> during the COVID-19 period is in light of lockdowns counterintuitive and needs a clearer discussion in the text. The authors state that it is due to transport from outside of China, but the quantified 4-10% of PM<sub>2.5</sub> transport into a Chinese region for polluted days and even the largest 40-66% regional contributions from transport during the lockdown, when local emission should be small, are no particularly convincing evidences, especially in light of the known poor model performance for PM<sub>2.5</sub> indicated by the authors.

Response:

Thanks for the suggestion. The polluted days are selected for “each receptor region” in China. Therefore, the large contribution from transboundary transport is only for some specific regions in China, e.g., Southwestern China. Also, the significant impacts from South and Southeast Asian emissions have been revealed in many previous studies.

We have now revised the sentences: “In this study, the most polluted day is defined as the day with the highest daily PM<sub>2.5</sub> concentration in February 2020 for each receptor region in China. The transport from outside of China only has a great impact on some specific regions in China. In Southwestern China, the relative contribution from ROW emissions, especially those from South and Southeast Asia, to the increment of PM<sub>2.5</sub> concentration during the most polluted days compared with normal days is more than 50%. It is consistent with the previous studies that emissions from South and Southeast Asia have an important impact on air quality in southwest China (Yang et al., 2017a; Zhu et al., 2016, 2017). For other receptor regions in China (Northeastern China, North China Plain, Eastern China, Southern China and Central-West China), PM<sub>2.5</sub> concentrations are largely contributed by local

emissions during the most polluted days compared with normal days. In the future with emissions reductions for better air quality in China, decreasing air pollution should consider aerosols from both Chinese local emissions and pollutant transport from outside of China.”

The results need a more compelling interpretation, making better use of the knowledge of the impact of the meteorological conditions on PM<sub>2.5</sub>, e.g., through a discussion in light of other studies. It would be useful to have a discussion section separate from the conclusions. This would allow to fully appreciate the limits and advances of this work compared to previous studies, and draw a clear and concise conclusion from this work.

Response:

Thanks for the suggestion. We have now included such context in the discussion section as follows: “Many studies have examined the importance of meteorology on regional air quality during the COVID-19 lockdown period and emphasized that, when meteorology is unfavorable, abrupt emissions reductions cannot avoid severe air pollutions (Le et al. 2020; Sulaymon et al. 2021; Shen et al. 2021). Through model simulations, Le et al. (2020) found that abnormally high humidity promotes the heterogeneous chemistry of aerosols, which have contributed to the increase of PM<sub>2.5</sub> by 12% in northern China during the city lockdown period. Sulaymon et al. (2021) found that significant increase in PM<sub>2.5</sub> concentrations caused by unfavorable meteorological conditions in Beijing-Tianjin-Hebei region during the lockdown period based on Community Multiscale Air Quality (CMAQ) model simulations. By analyzing the observational data and model simulations, Shen et al. (2021) reported that 50% of the pollution episodes during the COVID-19 lockdown in Hubei of China were due to the stagnant meteorological conditions. Huang et al. (2020) found that the stagnant air conditions and enhanced atmospheric oxidizing capacity caused a severe haze event during the same time period. In line with previous studies, we also revealed the stagnant air condition under the anomalous high pressure system in the most polluted day over the North China Plain. In addition to the meteorological conditions, the effect of foreign transport was also raised in this study causing aerosol pollution in southwestern China during COVID-19 outbreak.”

Specific comments

L. 51: “in December 2019” - give the time period of the outbreak in China

Response:

As the epidemic broke out one after another in different areas, the outbreak time is a continuous time. We have now revised the text as follows: “The coronavirus disease 2019 (COVID-19) has spread worldwide since December 2019 and resulted in more than one million cases within the first four months

(Sharma et al., 2020; Dong et al., 2020).”

L. 53-54: I recommend removing “was the first country” from the sentence since it is not relevant for the scientific content, but say instead when the measures began and ended since this is indeed relevant for the interpretation of your findings.

Response:

We have now revised the sentence to reflect this: “In order to curb the virus spread among humans, measures were taken by the Chinese government on January 23, 2020 to minimize the interaction among people, including strict isolation, prohibition of large-scale private and public gatherings, restriction of private and public transportation and even lockdown of cities (Tian et al., 2020; Wang et al., 2020).”

L. 62-63: revise sentence for clarity

Response:

We have now revised the sentence: “The estimated NO<sub>x</sub> emission in eastern China was reduced by 60-70%, of which 70-80% was related to the reduced road traffic and 20-25% was from industrial enterprises shutdown during the COVID-19 lockdown period. However, severe air pollution events still occurred in East China during the COVID-19 lockdown, even though the anthropogenic emissions were greatly reduced (Huang et al., 2020).”

L. 66: “change” -> changes

Response:

Revised.

L. 80-83: when did the haze occur? Does your simulation reproduce this event?

Response:

In the study of Huang et al. (2020), the severe air pollution events occurred on February 11, 2020. Our model reproduced the pollution event at the same time and have now included such context in the discussion as follows: “When the PM<sub>2.5</sub> pollution occurred in the North China Plain on February 11, 2020, which was also reported as the polluted day in observations (Huang et al., 2020), the concentration of PM<sub>2.5</sub> was 16.1 μg m<sup>-3</sup> higher than that in normal days.”

L. 114-116: If there are studies already, what does your work add to the previous knowledge?

Response:

In the original text, “few” studies have focused on aerosol transport pathways and source attribution in China during the COVID-19 pandemic. Since the studies about the air quality during COVID-19 are increasing, we have emphasized our study that “Our study provides source apportionment of

aerosols covering the whole China and quantifies the contribution from foreign transport for the first time in the case of COVID-19 emission reductions.”

L. 146: How many simulations did you perform over what time period?

Response:

By adding an additional simulation in the revised manuscript, we now have two simulations with aerosol tagging but different emission assumptions: “The anthropogenic emissions used in the baseline simulation are derived from the MEIC (Multi-resolution Emission Inventory of China) inventory (Zheng et al., 2018), referred to here as the Baseline experiment. While emissions for the other countries use the SSP (Shared Socioeconomic Pathways) 2–4.5 scenario data set under CMIP6 (the Coupled Model Intercomparison Project Phase 6). Emissions in year 2017 are used as the baseline during the simulation period considering the time limit of MEIC inventory. To better estimate the impact of restricted human activities on emission reductions owing to COVID-19 lockdown (referred to as Covid experiment), we updated China’s emission inventory from January to March 2020 based on the provincial total emission reduction ratio in Huang et al. (2020). Emissions from the transportation sector are decreased by 70%. The remaining emission reduction, by excluding transport reduction from the total emission reduction, are evenly distributed to other sectors, including industry, power plant, residential, international shipping and waste treatment from January to March 2020 compared to the baseline emission in 2017. Unless otherwise specified, all the results in this study are derived from the Covid experiment.”

L. 150-151: There should be an argument why emissions from SSP2-4.5 are used here, even though more recent global emission data has been created (e.g., Lamboll et al., 2020)

Response:

When we conducted the experiments, the latest global emission data has not been published. Applying the emissions from SSP2-4.5 can better compare with the simulations of CMIP6, which has been widely used in many previous studies (Lund et al. 2019; Lyakaremye et al. 2021).

L. 157-160: How were these emission estimates created? Please illustrate the results for the emissions and compare them to other new emission data. What is meant by „remaining reductions“?

Response:

The emission reductions due to COVID-19 lockdown were updated based on dynamic economic and industrial activity levels, which has been applied in the previous studies (Huang et al., 2020). Emissions from the transportation sector are decreased by 70%. The remaining emission reduction, by excluding transport reduction from the total emission reduction, are evenly distributed to other sectors, including industry, power plant, residential, international shipping

and waste treatment from January to March 2020 compared to the baseline emission in 2017.

L. 166: “from April 2019 to March 2020 repeatedly for six years” this needs more words to explain what you did. How did you do for instance the initialisation? What is meant by repeating the simulation for six years?

Response:

The simulations are integrated for 6 years with the first five years treated as model spin-up and the last year was analyzed.

L. 169: It would be more relevant to say which weeks had the most severe lockdowns and use this information to interpret the results.

Response:

The lockdown was first implemented on January 23 in Wuhan, China. Subsequently, other regions in China took measures, and the lockdown of the whole country lasted for at least three weeks varying in different regions.

L. 191: What motivates the choice of these regions?

Response:

The eight source areas are divided mainly according to the geographical location and subdivided on the basis of previous studies (Yang et al., 2017a).

L. 198-201: Were these nudged simulations to MERRA-2 as well? Then say so. Otherwise, it would be useful to say a few words on the performance of MERRA-2 over China as well.

Response:

Yes. Many studies have nudged the model wind fields toward the MERRA-2 reanalysis in China (Zhuang et al., 2018; Yang et al., 2017a).

L. 212: I appreciate and encourage the open communication of uncertainties in modeling. A 50% underestimation of PM<sub>2.5</sub> is large. Given your focus on PM<sub>2.5</sub> in this study, how can you nevertheless trust the simulation, especially taking into account that nitrate and ammonium are known to be poorly represented in the same model (L. 217)? You revisit this point in the last paragraph of the conclusions, but I also missed guidance for the concrete implication of it there.

Response:

We have now added the sentence to reflect this: “In majority of the climate models, the simulation of nitrate and ammonium aerosols are not included in the aerosol schemes, partly due to the complexity of calculation efficiency. For example, in many of the CMIP6 models, only two of them provide nitrate and ammonium mass mixing ratios. Many previous studies have evaluated the global climate models performance in reproducing aerosol concentrations (e.g., Fan et al., 2018; Shindell et al., 2013; Yang et al., 2017a,b). In general, the models can well simulate aerosols in North America and Europe but significantly underestimates aerosols in East Asia by about -36 to -58 %

compared with observations. It can lead to an underestimation of aerosols contributed by Chinese local emissions in magnitudes, but might not change the main conclusions of this study.”

L. 227: State here the three time periods and motivate this choice.

Response:

We now have added a description as follows. “Figure 3b presents spatial distributions of simulated mean column burden of PM<sub>2.5</sub> during the three time periods (‘Week 1’: January 30–February 5, ‘Week 2’: February 6–February 12 and ‘Week 3’: February 13–February 19), which had the largest number of newly-diagnosed COVID-19 cases.”

L. 230 - 236: Say relative to what you make the comparisons.

Response:

We have now revised the sentences: “Comparing to Week 3, Week 1 and Week 2 have higher PM<sub>2.5</sub> loading, with values in the range of 20–40 and 20–30 mg m<sup>-2</sup> in the North China Plain, Eastern China, and Southern China, while the PM<sub>2.5</sub> loading in Week 3 is relative lower than Week 1 and Week 2 with values ranging mostly from 10 to 20 mg m<sup>-2</sup>.”

L. 368: It would be helpful to state the date in the text, here and/or earlier.

Response:

We now have added a description as follows. “When the PM<sub>2.5</sub> pollution occurred in the North China Plain on February 11, 2020, which was also reported as the polluted day in observations (Huang et al., 2020), the concentration of PM<sub>2.5</sub> was 16.1 µg m<sup>-3</sup> higher than that in normal days.”

L. 273-374: 4-10% transport from outside of China on the most polluted day means that local emissions dominate. Maybe explicitly add the implication of your findings.

Response:

Thanks for the suggestion. We have now included such discussions as follows: “The transport from outside of China only has a great impact on some specific regions in China. In Southwestern China, the relative contribution from ROW emissions, especially those from South and Southeast Asia, to the increment of PM<sub>2.5</sub> concentration during the most polluted days compared with normal days is more than 50%. It is consistent with the previous studies that emissions from South and Southeast Asia have an important impact on air quality in southwest China (Yang et al., 2017a; Zhu et al., 2016, 2017). For other receptor regions in China (Northeastern China, North China Plain, Eastern China, Southern China and Central-West China), PM<sub>2.5</sub> concentrations are largely contributed by local emissions during the most polluted days compared with normal days. In the future with emissions reductions for better air quality in China, decreasing air pollution should consider aerosols from both

Chinese local emissions and pollutant transport from outside of China.”

Arrange the order of all figures following the order of references to them in the text.

Response:

Thank you for your reminding, we have reorganized the order of figures.

Figure 1: What time period is meant here?

Response:

The time period here refers to the three weeks of the study from January 30 to February 19, which had the largest number of newly-diagnosed COVID-19 cases.

Figure 2: What do the colors mean?

Response:

The color is to distinguish the different weeks. We have now moved this figure to the supplement.

Table 1: State the dates of the weeks.

Response:

We have now revised the sentences: “Table 1. Fractional contributions of emissions from nine tagged source regions (vertical axis) to mean PM<sub>2.5</sub> column burden in eight receptor regions (horizontal axis) during the three time periods (‘Week 1’: January 30–February 5, ‘Week 2’: February 6–February 12 and ‘Week 3’: February 13–February 19).”

Reference:

Fan, T., Liu, X., Ma, P.-L., Zhang, Q., Li, Z., Jiang, Y., Zhang, F., Zhao, C., Yang, X., Wu, F., and Wang, Y.: Emission or atmospheric processes? An attempt to attribute the source of large bias of aerosols in eastern China simulated by global climate models, *Atmos. Chem. Phys.*, 18, 1395–1417, <https://doi.org/10.5194/acp-18-1395-2018>, 2018.

Huang, X., Ding, A., Gao, J., Zheng, B., Zhou, D., Qi, X., Tang, R., Ren, C., Nie, W., Chi, X., Wang, J., Xu, Z., Chen, L., Li, Y., Che, F., Pang, N., Wang, H., Tong, D., Qin, W., Cheng, W., Liu, W., Fu, Q., Chai, F., Davis, S. J., Zhang, Q., He, K.: Enhanced secondary pollution offset reduction of primary emissions during COVID-19 lockdown in China, *National Science Review*, nwa137, <https://doi.org/10.1093/nsr/nwaa137>, 2020.

Le, T., Wang, Y., Liu, L., Yang, J., Yung, Y. L., Li, G., Seinfeld, J. H.: Unexpected air pollution with marked emission reductions during the COVID - 19 outbreak in China, *Science*, 369, 702–706, <https://doi.org/10.1126/science.abb7431>, 2020.

Lyakaremye, V., Zeng, G., Siebert, A., Yang, X.: Contribution of external

- forcings to the observed trend in surface temperature over Africa during 1901–2014 and its future projection from CMIP6 simulations, *Atmospheric Research*, 254, 105512, <https://doi.org/10.1016/j.atmosres.2021.105512>, 2021.
- Lund, M. T., Myhre, G., and Samset, B. H.: Anthropogenic aerosol forcing under the Shared Socioeconomic Pathways, *Atmos. Chem. Phys.*, 19, 13827–13839, <https://doi.org/10.5194/acp-19-13827-2019>, 2019.
- Shen, L., Zhao, T., Wang, H., Liu, J., Bai, Y., Kong, S., Zheng, H., Zhu, Y., Shu, Z.: Importance of meteorology in air pollution events during the city lockdown for COVID-19 in Hubei Province, Central China, *Sci. Total Environ.*, 754, 142227, <https://doi.org/10.1016/j.scitotenv.2020.142227>, 2021.
- Shindell, D. T., Lamarque, J.-F., Schulz, M., Flanner, M., Jiao, C., Chin, M., Young, P. J., Lee, Y. H., Rotstayn, L., Mahowald, N., Milly, G., Faluvegi, G., Balkanski, Y., Collins, W. J., Conley, A. J., Dalsoren, S., Easter, R., Ghan, S., Horowitz, L., Liu, X., Myhre, G., Nagashima, T., Naik, V., Rumbold, S. T., Skeie, R., Sudo, K., Szopa, S., Takemura, T., Voulgarakis, A., Yoon, J.-H., and Lo, F.: Radiative forcing in the ACCMIP historical and future climate simulations, *Atmos. Chem. Phys.*, 13, 2939–2974, <https://doi.org/10.5194/acp-13-2939-2013>, 2013.
- Sulaymon, I. D., Zhang, Y., Hopke, P. K., Hu, J., Zhang, Y., Li, L., Mei, X., Gong, K., Shi, Z., Zhao, B., Zhao, F.: Persistent high PM<sub>2.5</sub> pollution driven by unfavorable meteorological conditions during the COVID-19 lockdown period in the Beijing-Tianjin-Hebei region, China, *Environ. Res.*, 198, 111186, <https://doi.org/10.1016/j.envres.2021.111186>, 2021.
- Tian, H., Liu, Y., Li, Y., Wu, C., Chen, B., Kraemer, M.U.G., Li, B., Cai, J., Xu, B., Yang, Q., Wang, B., Yang, P., Cui, Y., Song, Y., Zheng, P., Wang, Q., Bjornstad, O.N., Yang, R., Grenfell, B.T., Pybus, O.G., Dye, C.: An investigation of transmission control measures during the first 50 days of the COVID-19 epidemic in China, *Science*, b6105 <https://doi.org/10.1126/science.abb6105>, 2020.
- Wang, P., Chen, K., Zhu, S., Wang, P., Zhang, H.: Severe air pollution events not avoided by reduced anthropogenic activities during COVID-19 outbreak, *Resources Conservation and Recycling*, 158, 104814, <https://doi.org/10.1016/j.resconrec.2020.104814>, 2020.
- Yang, Y., Wang, H., Smith, S. J., Ma, P. L., Rasch, P. J.: Source attribution of black carbon and its direct radiative forcing in China, *Atmospheric Chemistry and Physics*, 17, 4319–4336, <https://doi.org/10.5194/acp-17-4319-2017>, 2017a.
- Yang, Y., Wang, H., Smith, S. J., Easter, R., Ma, P. L., Qian, Y., Yu, H., Li, C., Rasch, P. J.: Global source attribution of sulfate concentration and direct and indirect radiative forcing, *Atmospheric Chemistry and Physics*, 17, 8903–8922, <https://doi.org/10.5194/acp-17-8903-2017>, 2017b.
- Zheng, B., Tong, D., Li, M., Liu, F., Hong, C., Geng, G., Li, H., Li, X., Peng, L.,



- Qi, J., Yan, L., Zhang, Y., Zhao, H., Zheng, Y., He, K., and Zhang, Q.: Trends in China's anthropogenic emissions since 2010 as the consequence of clean air actions, *Atmospheric Chemistry and Physics*, 18, 14095–14111, <https://doi.org/10.5194/acp-18-14095-2018>, 2018.
- Zhuang, B. L., Li, S., Wang, T. J., Liu, J., Chen, H. M., Chen, P. L., Li, M. M., Xie, M.: Interaction between the Black Carbon Aerosol Warming Effect and East Asian Monsoon Using RegCM4, *J. Climate*, 31(22), 9367–9388, <https://doi.org/10.1175/JCLI-D-17-0767.1>, 2018.
- Zhu, J., Xia, X., Che, H., Wang, J., Zhang, J., Duan, Y.: Study of aerosol optical properties at Kunming in southwest China and longrange transport of biomass burning aerosols from North Burma, *Atmos. Res.*, 169, 237–247, <https://doi.org/10.1016/j.atmosres.2015.10.012>, 2016.
- Zhu, J., Xia, X., Wang, J., Zhang, J., Wiedinmyer, C., Fisher, J. A., Keller, C. A.: Impact of Southeast Asian smoke on aerosol properties in Southwest China: First comparison of model simulations with satellite and ground observations, *J. Geophys. Res. Atmos.*, 122, 3904–3919, <https://doi.org/10.1002/2016JD025793>, 2017.

## Manuscript # acp-2021-328

### Responses to Referee #2

The authors investigated aerosol transport pathways in China during COVID-19. They established the source-receptor relationships among various regions of China using the CAM5 model with the capability of aerosol source tagging. The model system was developed by the same group of this paper and was evaluated in their previous studies. This work suggests that local emissions contribute largely to the severe aerosol pollution in North China Plain and Eastern China during COVID along with moderate impacts from unfavorable meteorological conditions. Overall, this paper reads well and provides interesting results, which could benefit the design of air pollution regulation strategies in China. I have two major concerns about the manuscript in its current form, which need to be resolved before it can be accepted for publication.

We thank the editor for all the insightful comments. Below, please see our point-by-point response (in blue) to the specific comments and suggestions and the changes that have been made to the manuscript, in effort to take into account all the comments raised here.

The first problem is that the CAM5 model used in this work cannot simulate nitrate and ammonium aerosols, while these compositions account for a large proportion of aerosols over China currently. Please provide detailed explanations and discussions on how this model deficiency could impact the main conclusions of this work.

Response:

Thanks for the suggestion. We have now added the following sentences in the discussion section: "In majority of the climate models, the simulation of nitrate and ammonium aerosols are not included in the aerosol schemes, partly due to the complexity of calculation efficiency. For example, in many of the CMIP6 models, only two of them provide nitrate and ammonium mass mixing ratios. Many previous studies have evaluated the global climate models in reproducing aerosol concentrations (e.g., Fan et al., 2018; Shindell et al., 2013; Yang et al., 2017a, b). In general, the models can well simulate aerosols in North America and Europe but significantly underestimates aerosols in East Asia by about -36 to -58 % compared with observations. It can lead to an underestimation of aerosols contributed by Chinese local emissions in magnitudes, but might not change the main conclusions of this study."

The second problem is that the focus of this work is the aerosol source

attribution during COVID. However, the authors did not discuss much the special findings in this special period. Compared to previous literature, are there any novel results and conclusions of the contributions from local/nonlocal sources to aerosol pollutions during this period with low emission levels? And what's the implication for air pollution control policies in China, especially considering that the anthropogenic emissions will be rapidly reduced in the future?

Response:

Thanks for the suggestion. We have now included such context in the discussion section as follows: "Source tagging and apportionment is an effective way to establish aerosol source-receptor relationships, which is conducive to both scientific research and emission control strategies (Yu et al., 2012). Previous studies only focused on regional transport of aerosols, very few studies have explored the aerosol transport pathways and source attribution covering the whole China during the COVID-19 pandemic. The COVID-19 pandemic disrupted human activities and lead to abrupt reductions in anthropogenic emissions. This study first investigated the source contributions to PM<sub>2.5</sub> over various regions covering the whole China during the COVID-19 pandemic. We pay attention not only to local emissions, but also to the impacts from regional and foreign transport of aerosols."

In the revised manuscript, we added an additional experiment to better reflect variations of contributions from local/nonlocal sources to aerosol pollutions during this period with low emission levels. "The anthropogenic emissions used in the baseline simulation are derived from the MEIC (Multi-resolution Emission Inventory of China) inventory (Zheng et al., 2018), referred to here as the Baseline experiment. While emissions for the other countries use the SSP (Shared Socioeconomic Pathways) 2–4.5 scenario data set under CMIP6 (the Coupled Model Intercomparison Project Phase 6). Emissions in year 2017 are used as the baseline during the simulation period considering the time limit of MEIC inventory."

"To highlight the roles of regional and foreign transport, the differences between Covid and Baseline simulations in relative contributions to PM<sub>2.5</sub> burden from local, region (RCN) and foreign (ROW) emissions are given in Figure S1. During the COVID-19 period, the local and RCN emission contributions to PM<sub>2.5</sub> were 1–4% lower than that in Base experiment over NCP and NEC. In Eastern China, the contribution from the local emissions decreased by 3–4% compared with Base experiment, while the contribution from ROW increased by more than 5%. In Southern China, 50–70% of the PM<sub>2.5</sub> burden is contributed by emissions from ROW in Base experiment. During the COVID-19 period with low emission levels, the contribution from ROW to PM<sub>2.5</sub> burden in Southern China had an increase of more than 5%. It indicates that the important role of transboundary transport needs to be considered when controlling local emissions to improve air quality in the near future."

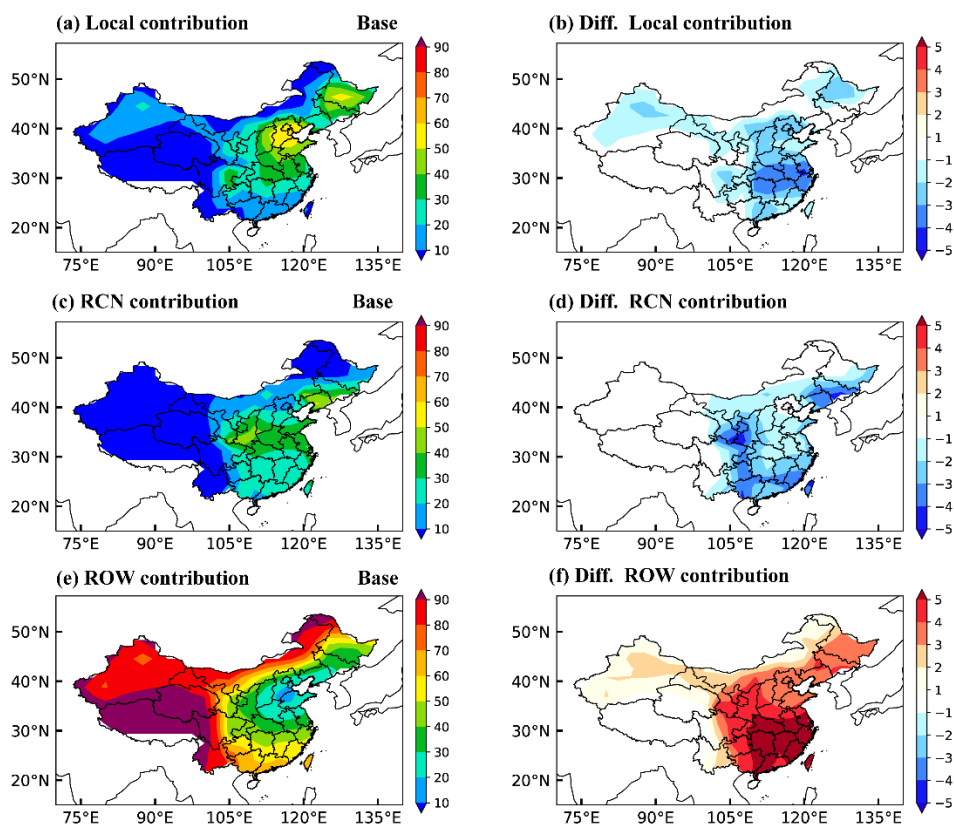


Figure S1. Relative contributions (%) in Baseline simulation (left) and differences in relative contributions (%) between Covid and Baseline simulations (right) of local emissions (top), the emissions from the rest of China (RCN) (middle) and all sources outside China (rest of the world, ROW) (bottom) to PM<sub>2.5</sub> column burden in February 2020.

Reference:

Fan, T., Liu, X., Ma, P.-L., Zhang, Q., Li, Z., Jiang, Y., Zhang, F., Zhao, C., Yang, X., Wu, F., and Wang, Y.: Emission or atmospheric processes? An attempt to attribute the source of large bias of aerosols in eastern China simulated by global climate models, *Atmos. Chem. Phys.*, 18, 1395–1417, <https://doi.org/10.5194/acp-18-1395-2018>, 2018.

Shindell, D. T., Lamarque, J.-F., Schulz, M., Flanner, M., Jiao, C., Chin, M., Young, P. J., Lee, Y. H., Rotstajn, L., Mahowald, N., Milly, G., Faluvegi, G., Balkanski, Y., Collins, W. J., Conley, A. J., Dalsoren, S., Easter, R., Ghan, S., Horowitz, L., Liu, X., Myhre, G., Nagashima, T., Naik, V., Rumbold, S. T., Skeie, R., Sudo, K., Szopa, S., Takemura, T., Voulgarakis, A., Yoon, J.-H., and Lo, F.: Radiative forcing in the ACCMIP historical and future climate simulations, *Atmos. Chem. Phys.*, 13, 2939–2974, <https://doi.org/10.5194/acp-13-2939-2013>, 2013.

Yang, Y., Wang, H., Smith, S. J., Ma, P. L., Rasch, P. J.: Source attribution of

black carbon and its direct radiative forcing in China, *Atmospheric Chemistry and Physics*, 17, 4319–4336, <https://doi.org/10.5194/acp-17-4319-2017>, 2017a.

Yang, Y., Wang, H., Smith, S. J., Easter, R., Ma, P. L., Qian, Y., Yu, H., Li, C., Rasch, P. J.: Global source attribution of sulfate concentration and direct and indirect radiative forcing, *Atmospheric Chemistry and Physics*, 17, 8903–8922, <https://doi.org/10.5194/acp-17-8903-2017>, 2017b.

Yu, H. B., Remer, L. A., Chin, M., Bian, H. S., Tan, Q., Yuan, T. L., Zhang, Y.: Aerosols from overseas rival domestic emissions over North America, *Science*, 337, 566–569, <https://doi.org/10.1126/science.1217576>, 2012.

Zheng, B., Tong, D., Li, M., Liu, F., Hong, C., Geng, G., Li, H., Li, X., Peng, L., Qi, J., Yan, L., Zhang, Y., Zhao, H., Zheng, Y., He, K., and Zhang, Q.: Trends in China's anthropogenic emissions since 2010 as the consequence of clean air actions, *Atmospheric Chemistry and Physics*, 18, 14095–14111, <https://doi.org/10.5194/acp-18-14095-2018>, 2018.

1 **Aerosol transport pathways and source attribution in China**  
2 **during the COVID-19 outbreak**

3

4

5 Lili Ren<sup>1</sup>, Yang Yang<sup>1\*</sup>, Hailong Wang<sup>2</sup>, Pinya Wang<sup>1</sup>, Lei Chen<sup>1</sup>, Jia

6 Zhu<sup>1</sup>, Hong Liao<sup>1</sup>

7

8

9

10

11 <sup>1</sup>Jiangsu Key Laboratory of Atmospheric Environment Monitoring and Pollution  
12 Control, Jiangsu Collaborative Innovation Center of Atmospheric Environment and  
13 Equipment Technology, School of Environmental Science and Engineering, Nanjing  
14 University of Information Science and Technology, Nanjing, Jiangsu, China

15 <sup>2</sup>Atmospheric Sciences and Global Change Division, Pacific Northwest National  
16 Laboratory, Richland, Washington, USA

17

18

19

20

21 \*Correspondence to [yang.yang@nuist.edu.cn](mailto:yang.yang@nuist.edu.cn)

22

## 23 **Abstract**

24 Due to the coronavirus disease 2019 (COVID-19) pandemic, human  
25 activities and industrial productions were strictly restricted during January-  
26 March 2020 in China. Despite the fact that anthropogenic aerosol  
27 emissions largely decreased, haze events still occurred. Characterization of  
28 aerosol transport pathways and attribution of aerosol sources from specific  
29 regions are beneficial to the air quality and pandemic control strategies.  
30 This study establishes source-receptor relationships in various regions  
31 [covering the whole](#) China during the COVID-19 outbreak based on the  
32 Community Atmosphere Model version 5 with Explicit Aerosol Source  
33 Tagging (CAM5-EAST). Our analysis shows that PM<sub>2.5</sub> burden over the  
34 North China Plain between January 30 and February 19 is [largely mostly](#)  
35 contributed by local emissions (40–66%). For other regions in China, PM<sub>2.5</sub>  
36 burden is largely contributed from non-local sources. During the [most](#)  
37 polluted days of COVID-19 outbreak, local emissions within North China  
38 Plain and Eastern China, respectively, contribute 66% and 87% to the  
39 increase in surface PM<sub>2.5</sub> concentrations. This is associated with the  
40 anomalous mid-tropospheric high pressure at the location of climatological  
41 East Asia trough and the consequently weakened winds in the lower  
42 troposphere, leading to the local aerosol accumulation. The emissions  
43 outside China, especially [those](#) from South and Southeast Asia, contribute  
44 over 50% to the increase in PM<sub>2.5</sub> concentration in Southwestern China

45 through transboundary transport during the [most](#) polluted day. As the  
46 reduction in emissions in the near future, aerosols from long-range  
47 transport together with unfavorable meteorological conditions are  
48 increasingly important to regional air quality and need to be taken into  
49 account in clean air plans.



## 50 1. Introduction

51 The coronavirus disease 2019 (COVID-19) ~~had an outbreak in China~~  
52 ~~in~~ has spread worldwide since December 2019. ~~It has~~ and resulted in more  
53 than one million cases within the first four months ~~worldwide~~ (Sharma et  
54 al., 2020; Dong et al., 2020). In order to curb the virus spread among  
55 humans, ~~China was the first country to take dramatic~~ measures were taken  
56 by the Chinese government on January 23, 2020 to minimize the  
57 interaction among people, including strict isolation, prohibition of large-  
58 scale private and public gatherings, restriction of private and public  
59 transportation and even lockdown of cities (Tian et al., 2020; Wang et al.,  
60 2020). The estimated NO<sub>x</sub> emission in eastern China was reduced by 60-  
61 70%, of which 70-80% was related to the reduced road traffic and 20-25%  
62 was from industrial enterprises shutdown during the COVID-19 lockdown  
63 period ~~(Huang et al., 2020).~~ However, severe air pollution events still  
64 occurred in East China during the COVID-19 lockdown. ~~It is of great~~  
65 ~~concern that why severe air pollution was not avoided by decreasing, even~~  
66 though the anthropogenic emissions were greatly reduced (Huang et al.,  
67 2020). The unprecedented large-scale restrictions resulting from the  
68 COVID-19 epidemic provide an opportunity to research the relationship  
69 between dramatic anthropogenic emission reductions and air quality  
70 ~~change~~ changes (e.g., Bao et al., 2020; Li et al., 2020; Wang et al., 2020).  
71 Bao et al. (2020) reported that, during the COVID-19 lockdown period, the

72 air quality index (AQI) and the PM<sub>2.5</sub> (particulate matter less than 2.5 μm  
73 in diameter) concentration were decreased by 7.8% and 5.9 %, respectively,  
74 on average in 44 cities in northern China, mainly due to travel restrictions.  
75 By applying the WRF-CAMx model together with air quality monitoring  
76 data, Li et al. (2020) revealed that although primary particle emissions were  
77 reduced by 15%–61% during the COVID-19 lockdown over the Yangtze  
78 River Delta Region, the daily mean concentration of PM<sub>2.5</sub> was still  
79 relatively high, reaching up to 79 μg m<sup>-3</sup>. Wang et al. (2020) found that the  
80 relative reduction in PM<sub>2.5</sub> precursors was twice as much as the reduction  
81 in PM<sub>2.5</sub> concentration, in part due to the unfavorable meteorological  
82 conditions during the COVID-19 outbreak in China that led to the  
83 formation of the heavy haze. Huang et al. (2020) and Le et al. (2020)  
84 reported that stagnant air conditions, high atmospheric humidity, and  
85 enhanced atmospheric oxidizing capacity led to a severe haze event in  
86 northern China during the COVID-19 pandemic.

87 Aerosols are main air pollutants that play important roles in the  
88 atmosphere due to their adverse effects on air quality, visibility (Vautard et  
89 al., 2009; Watson, 2002), human health (Lelieveld et al., 2019; Heft-Neal  
90 et al., 2018), the Earth's energy balance, and regional and global climate  
91 (Ramanathan et al., 2001; Anderson et al., 2003; Wang et al., 2020; Smith  
92 et al., 2020). With the rapid development in recent decades, China has  
93 experienced severe air pollutions that damage human health and cause

94 regional climate change (Chai et al., 2014; Liao et al., 2015; Fan et al.,  
95 2020). In order to control air pollution, the Chinese government issued and  
96 implemented the Air Pollution Prevention and Control Action Plan in 2013  
97 (China State Council, 2013). Although emissions in China have decreased  
98 significantly in recent years (Zheng et al., 2018), aerosols transported from  
99 other source regions could add on top of local emissions (Yang et al., 2017a,  
100 2018a; Ren et al., 2020). Therefore, it is important to understand the  
101 relative effects of local emissions and regional transport on aerosols in  
102 China.

103 Source tagging and apportionment is an effective way to establish  
104 aerosol source-receptor relationships, which is conducive to both scientific  
105 research and emission control strategies (Yu et al., 2012). By applying the  
106 Particulate Source Apportionment Technology in CAMx model, Xue et al.  
107 (2014) found that the contributions of regional transport to annual average  
108  $PM_{2.5}$  concentrations in Hainan, Shanghai, Jiangsu, Zhejiang, Jilin and  
109 Jiangxi provinces of China are more than 45%. By adding a chemical tracer  
110 into the WRF model, Wang et al. (2016) studied the sources of black carbon  
111 (BC) aerosol in Beijing and reported that about half of BC in Beijing came  
112 from the central North China Plain. Liu et al. (2017) applied WRF-Chem  
113 model and showed that Foshan, Guangzhou and Dongguan, respectively,  
114 with relatively high emissions contributed 14%, 13% and 10% to the  
115 regional mean  $PM_{2.5}$  concentration in the Pearl River Delta.

116 Currently, ~~many previous studies only focused on regional transport of~~  
117 ~~aerosols, very few~~ studies have ~~investigated the impact of reduced human~~  
118 ~~activity on regional air quality, as a result of the COVID-19 outbreak. Few~~  
119 ~~studies have focused on~~ explored the aerosol transport pathways and source  
120 attribution ~~in~~ covering the whole China during the COVID-19 pandemic. In  
121 this study, the global aerosol-climate model CAM5 (Community  
122 Atmosphere Model, version 5) equipped with an Explicit Aerosol Source  
123 Tagging (CAM5-EAST) is employed to quantify source-receptor  
124 relationships and transport pathways of aerosols during the COVID-19  
125 outbreak in China. We also provide model evaluations of PM<sub>2.5</sub>  
126 concentrations against observations made during the COVID-19 outbreak.  
127 With the aerosol source tagging technique, source region contributions to  
128 PM<sub>2.5</sub> column burden over various receptor regions and transport pathways  
129 in China are analyzed. The source contributions to the changes in near-  
130 surface PM<sub>2.5</sub> in ~~the most~~ polluted days compared to the monthly means  
131 during February 2020 are also quantified. ~~This paper~~ Our study provides  
132 source apportionment of aerosols ~~in~~ covering the whole China ~~during~~  
133 ~~the~~ and quantifies the contribution from foreign transport for the first time  
134 ~~in the case of~~ COVID-19 emission reductions, which is beneficial to the  
135 investigation of policy implications for future air pollution control.

## 136 **2. Methods**

### 137 **2.1 Model description and experimental setup**

138 The CAM5 model is applied to estimate the PM<sub>2.5</sub> changes during the  
139 COVID-19 period. ~~In CAM5~~, which is the atmospheric component of the  
140 earth system model CESM (Community Earth System Model, Hurrell et  
141 al., 2013). In this study, major aerosol species including sulfate, BC,  
142 primary organic matter (POM), secondary organic aerosol (SOA), sea salt,  
143 and mineral dust, are represented by three lognormal size modes (i.e.,  
144 Aitken, accumulation, and coarse modes) of the modal aerosol module  
145 (MAM3) (Liu et al., 2012). The detailed aerosol representation in CAM5  
146 was provided in Liu et al. (2012) and Wang et al. (2013). The aerosol  
147 mixing states consider both internal mixed (within a same mode) and  
148 external mixed (between modes). On top of the default CAM5, additional  
149 modifications that improve the representation of aerosol wet scavenging  
150 and convective transport (Wang et al., 2013) are also included in the model  
151 version used for this study.

152 In this study, simulations were conducted with a horizontal resolution  
153 of  $1.9^\circ \times 2.5^\circ$  and 30 vertical layers up to 3.6 hPa in year 2020.  
154 ~~Anthropogenic~~The anthropogenic emissions used in Chinathe baseline  
155 simulation are derived from the MEIC (Multi-resolution Emission  
156 Inventory of China) inventory (Zheng et al., 2018). ~~while~~, referred to here  
157 as the Baseline experiment. While emissions for the other countries use the  
158 SSP (Shared Socioeconomic Pathways) 2–4.5 scenario data set under  
159 CMIP6 (the Coupled Model Intercomparison Project Phase 6). Emissions

160 in year 2017 are used as the baseline during the simulation period  
161 considering the time limit of MEIC inventory. To better estimate the impact  
162 of restricted human activities on emission reductions owing to COVID-19  
163 lockdown, (referred to as Covid experiment), we updated China's emission  
164 inventory from January to March 2020 based on the provincial total  
165 emission reduction ratio in Huang et al. (2020). Emissions from the  
166 transportation sector are decreased by 70% ~~and the~~%. The remaining  
167 reduction emission reduction, by excluding transport reduction from the  
168 total emission reduction, are evenly distributed to other sectors, including  
169 industry, power plant, residential, international shipping and waste  
170 treatment from January to March 2020 compared to the baseline emission  
171 in 2017. Unless otherwise specified, all the results in this study are derived  
172 from the Covid experiment.

173 The sea surface temperature, sea ice concentrations, solar radiation and  
174 greenhouse gas concentrations are fixed at present-day climatological  
175 levels. To capture the large-scale atmospheric circulations during the  
176 COVID-19, we nudge the model wind fields toward the MERRA-2  
177 (Modern-Era Retrospective Analysis for Research and Applications,  
178 version 2) reanalysis (Gelaro et al., 2017) from April 2019 to March 2020  
179 repeatedly for six years. Only model results from the last year are used to  
180 represent year 2020. with the first five years as model spin-up. In this study,  
181 we analyze the transport pathways and source attribution of aerosols during

182 the three weeks that had the largest number of newly-diagnosed COVID-  
183 19 cases (Fig. [2S1](#), hereafter referred to as the ‘Week 1’: January 30–  
184 February 5, ‘Week 2’: February 6–February 12 and ‘Week 3’: February 13–  
185 February 19), when unexpected hazardous air pollution events also  
186 occurred during this time period ([Huang et al., 2020](#); [Le et al., 2020](#)).

## 187 **2.2 Explicit aerosol source tagging and source regions**

188 To examine the source apportionment of aerosols in China, the Explicit  
189 Aerosol Source Tagging (EAST) technique was implemented in CAM5,  
190 which has been utilized in many aerosol source attribution studies (e.g.,  
191 Wang et al., 2014; Yang et al., 2017a, b, 2018a, b, c, 2020; Ren et al., 2020).  
192 Different from the emission sensitivity method that assumes a linear  
193 response to emission perturbation and the traditional backward trajectory  
194 method, aerosols from each tagged region or sector are calculated  
195 independently in EAST within one single simulation. Without relying on a  
196 set of model simulations with emission perturbations or assuming constant  
197 decaying rate, EAST is more accurate and time-saving than the source  
198 apportionment method mentioned above. In addition to the sulfate, BC and  
199 POM species that were tagged in previous studies (e.g., Yang et al., 2020),  
200 SOA and precursor gas are now also tagged in the EAST. These types of  
201 aerosols from independent source regions and sectors can be explicitly  
202 tagged and tracked simultaneously. In this study, focusing on the aerosols  
203 in China during the COVID-19 outbreak period, the domestic aerosol and

204 precursor emissions ~~are divided into~~from eight geographical source regions  
205 (Fig. 1), including Northeastern China (NEC), North China Plain (NCP),  
206 Eastern China (ESC), Southern China (STC), Central-West China (CWC),  
207 Southwestern China (SWC), Northwestern China (NWC) and the  
208 Himalayas and Tibetan Plateau (HTP), and the rest of the world (ROW)  
209 emissions), are tagged separately.

### 210 **3. Model evaluation**

211 Many previous studies have assessed the spatial distribution and  
212 seasonal to decadal variations in aerosol concentrations in China and  
213 worldwide simulated by CAM5 with the observations (e.g., Wang et al.,  
214 2013; Yang et al., 2017a,b, 2018b,c, 2020). In order to evaluate the model's  
215 performance in simulating aerosols during the COVID-19 outbreak period  
216 in China, the surface concentrations of PM<sub>2.5</sub>, estimated as the sum of  
217 sulfate, BC, POM and SOA for model results, during the analyzed time  
218 periods are compared with measurements from the China National  
219 Environmental Monitoring Center (CNEMC), as shown in Fig. [3a2a](#). The  
220 model reasonably reproduces the overall spatial distribution of near-  
221 surface PM<sub>2.5</sub> concentrations during the three time periods, with high  
222 values in the North China Plain and low values in western China. However,  
223 as reported in many CAM5 model studies (e.g., Yang et al., 2017a,b), the  
224 model underestimates the PM<sub>2.5</sub> concentrations with normalized mean  
225 biases (NMB) of -55%~-49%, compared to the available site observations



226 (Fig. [S1S2](#)). The discrepancies are related to coarse-resolution model  
227 sampling bias relative to the observational sites, uncertainties in aerosol  
228 emissions, wet removal, and gas-particle exchange. In addition, the model  
229 version used in this study is not able to simulate nitrate and ammonium  
230 aerosols, which are also the main components of PM<sub>2.5</sub> (Kong et al., 2020;  
231 Xu et al., 2019).

232 The long-distance transport of aerosols mainly occurs in the upper  
233 troposphere rather than near the surface (Hadley et al., 2007; Zhang et al.,  
234 2015). Aerosols are lifted from the atmospheric boundary layer of the  
235 emission source regions to the free troposphere and then undergo the  
236 transboundary and intercontinental transport effectively driven by the  
237 upper tropospheric circulations. Therefore, it is helpful to analyze the  
238 relative contributions of local and non-local sources by focusing on the  
239 column burden of aerosols. Figure [3b2b](#) presents spatial distributions of  
240 simulated mean column burden of PM<sub>2.5</sub> during the three time periods:  
241 [‘Week 1’: January 30–February 5, ‘Week 2’: February 6–February 12 and](#)  
242 [‘Week 3’: February 13–February 19\), which had the largest number of](#)  
243 [newly-diagnosed COVID-19 cases](#). The contrast in column burden does  
244 not differ significantly from that of near-surface concentrations. [Among the](#)  
245 [three time periods](#) [Comparing to Week 3](#), Week 1 and Week 2 have higher  
246 PM<sub>2.5</sub> loading, with values in the range of 20–40 and 20–30 mg m<sup>-2</sup> in the  
247 North China Plain, Eastern China, and Southern China, while the PM<sub>2.5</sub>

248 loading in Week 3 is relative lower with [than Week 1 and Week 2 with](#)  
249 values ranging mostly from 10 to 20 mg m<sup>-2</sup>. Note that the column burden  
250 of PM<sub>2.5</sub> in South and Southeast Asia is higher than 20 mg m<sup>-2</sup> in three time  
251 periods and reaches up to 50 mg m<sup>-2</sup> in Week 2, which potentially  
252 influences aerosol concentrations in China through transboundary  
253 transport.

#### 254 **4. Transport Pathways**

255 The explicit aerosol tagging technique can clearly identify the transport  
256 pathways of aerosols moving from their source regions to their destination.

257 Figure [43](#) shows the spatial distribution of mean column burden of  
258 simulated PM<sub>2.5</sub> originating from the six tagged source regions in central  
259 and eastern China and outside of China during the three time periods.  
260 Aerosols and/or precursor gases emitted from the various regions follow  
261 quite different transport pathways determined by their source locations,  
262 meteorological conditions, emission injection height, and physical and  
263 chemical characteristics of aerosol species. Aerosols from Northeastern  
264 China are transported southeastward by the northwesterly winds (Fig. 1b).  
265 From the North China Plain, aerosols can be transported either southward  
266 reaching Eastern, Southern and Southwestern China during Week 1 or  
267 across east coast of China to the oceanic region during Week 2-3. Aerosols  
268 originating from Eastern China move straight to Southwestern and  
269 Southern China during Week 1-2, while they also entered the North China

270 Plain during Week 2-3. Aerosols emitted from Southern China and Central-  
271 West China have no obvious transport due to their relatively weak  
272 emissions. In addition to the local impact, emissions from Southwestern  
273 China affect mostly the Southern China and Eastern China. Air parcels with  
274 high levels of  $PM_{2.5}$  from South and Southeast Asia moved into  
275 Southwestern, Southern and Eastern China and even the North China Plain  
276 during the three time periods.

277 The vertical distributions of  $PM_{2.5}$  emitted from six major tagged  
278 source regions are shown in Figs. [S2S3](#) and [S3S4](#). The  $PM_{2.5}$  has much  
279 higher concentrations in the lower troposphere and decreases with  
280 increasing height. During Week 1-2, owing to the presence of high  $PM_{2.5}$   
281 loadings, a stronger vertical mixing and transport brought more  $PM_{2.5}$  to  
282 the upper troposphere compared to that during Week 3. High  
283 concentrations of  $PM_{2.5}$  originating from the North China Plain extended  
284 southeastward by strong northwesterly winds. Weak winds over Eastern  
285 China led to accumulations of  $PM_{2.5}$  within this region, which is consistent  
286 with the findings in Yang et al. (2017a). Strong southwesterly winds in the  
287 south of Southwestern China and weak winds in the north of this region  
288 produced convergences and updrafts that lift aerosols up to 700 hPa.

289 Considering that the emissions outside China contribute greatly to  
290  $PM_{2.5}$  concentrations in Southwestern China through transboundary  
291 transport (Yang et al., 2017a) and aerosols from East Asia can be

292 transported to the North Pacific and even North America (Yu et al., 2008;  
293 Yang et al., 2018c), it is of great importance to study the inflow and outflow  
294 of PM<sub>2.5</sub> across the boundaries of China. Figures 54 and 65 show the  
295 vertical distribution of PM<sub>2.5</sub> concentrations resulting from emissions  
296 within and outside China over 29°N, 88°E and 21°N around the south  
297 boundaries (cross-sections (CS) 1-3 in Fig. 1a) and 123° E around the east  
298 boundary (CS 4 in Fig. 1a) of the mainland of China. Over the southern  
299 border, PM<sub>2.5</sub> concentrations are more influenced by transboundary  
300 transport of aerosols from ROW than those originating from domestic  
301 emissions. The high concentrations of PM<sub>2.5</sub> from South and Southeast  
302 Asia are lifted into the free atmosphere of the Tibetan Plateau and Yun-Gui  
303 Plateau, and then transported to Southern and Southwestern China by  
304 southwesterly winds. Over the North China Plain and Eastern China,  
305 northwesterly winds at 35-45° N and southwesterly winds at 25-35° N  
306 cause aerosols to accumulate in the lower atmosphere and then export  
307 across east border of China below 700 hPa.

## 308 **5. Source apportionment of PM<sub>2.5</sub> in China during the COVID-19**

### 309 **5.1 Source contributions to PM<sub>2.5</sub> burden**

310 Figure 76 shows the simulated relative contributions in percentage to  
311 PM<sub>2.5</sub> column burden from local source emissions, regional transport from  
312 the untagged regions of China (rest of China, RCN) and rest of the world  
313 (ROW). Over the North China Plain, where emissions are relatively high,

314 PM<sub>2.5</sub> column burden is dominated by local emissions during the three time  
315 periods. In contrast, regions with relative low emissions are mainly  
316 affected by nonlocal sources, especially by foreign contributions.  
317 Emissions from the ROW contribute a large amount to PM<sub>2.5</sub> burden over  
318 Northeastern, Southern, Central-West, Southwestern, Northwestern China  
319 and the Tibetan Plateau. PM<sub>2.5</sub> burden in Eastern China is greatly  
320 contributed by the sources from RCN, especially in Week 1 when regional  
321 transport of PM<sub>2.5</sub> from the North China Plain is relatively strong (Fig.  
322 [S3S4](#)).

323 Table 1 summarizes the contributions of tagged source regions to the  
324 PM<sub>2.5</sub> burden over different receptor regions in China. In Northeastern  
325 China, 36%-43% of the PM<sub>2.5</sub> column burden comes from local emissions,  
326 while a larger portion (39%-54%) is contributed by emissions from ROW  
327 during the three time periods. The impacts of nonlocal sources within  
328 China on PM<sub>2.5</sub> burden are relatively low in Northeastern China during  
329 Week 1 with the contribution of less than 5%, while RCN is responsible for  
330 23% and 25% during Week 2 and Week 3, respectively.

331 In the North China Plain, the majority of the PM<sub>2.5</sub> burden is attributed  
332 to local emissions in all cases, with local contributions in a range of 40–  
333 66%. Emissions from the North China Plain also produce a widespread  
334 impact on PM<sub>2.5</sub> over its neighboring regions. The sources from North  
335 China Plain account for 14–33% of the PM<sub>2.5</sub> burden in Eastern China and

336 7–23% in Southern China during the three time periods.

337 In Eastern China, local emissions account for 27–40% of PM<sub>2.5</sub> column  
338 burden, while ROW contributes 20–45%. Southern China and Central-  
339 West China have 13–18% and 25–31% of local source contributions,  
340 respectively, whereas 37–64% are due to emissions from outside China in  
341 these two regions. In Southwestern China, 15–18% of the PM<sub>2.5</sub> burden  
342 originates from local emissions and 7–24% is from RCN. ROW emissions  
343 play important roles in affecting PM<sub>2.5</sub> burden over this region, with  
344 relative contributions in a range of 59–78% during the three time periods,  
345 which is associated with the transboundary transport by southwesterly  
346 winds. PM<sub>2.5</sub> burden over the Northwestern China and Himalayas and  
347 Tibetan Plateau with relatively low local emissions are strongly influenced  
348 by nonlocal sources, where more than 70% of the PM<sub>2.5</sub> burden originates  
349 from emissions outside China.

## 350 **5.2 Aerosol source attribution during polluted days**

351 In spite of the large reductions in emissions, severe air pollution events  
352 still occurred in China during the COVID-19 lockdown. Source attribution  
353 of PM<sub>2.5</sub> during polluted days in China has policy implications for future  
354 air pollution control. In Beijing, capital of China over the North China  
355 Plain, a serious haze event happened from February 11 to 13, 2020 during  
356 the COVID-19 outbreak period according to observations released by  
357 CNEMC. CAM5-EAST reproduced the polluted day on February 11 over

358 the North China Plain. In this study, the most polluted day is defined as the  
359 day with the highest daily PM<sub>2.5</sub> concentration in February 2020 for each  
360 receptor region in China. Figure 87 presents the composite differences in  
361 near-surface PM<sub>2.5</sub> concentrations and 850 hPa wind fields between [the](#)  
362 [most](#) polluted [daysday](#) and normal days (all days in February 2020) for  
363 each receptor region. The local and nonlocal source contributions to the  
364 PM<sub>2.5</sub> differences are summarized in Fig. 98.

365 Unexpectedly, near-surface PM<sub>2.5</sub> concentrations in the North China  
366 Plain and Eastern China experienced remarkable increases during the [same](#)  
367 [most](#) polluted [daysday](#) of COVID-19 lockdown. The simulated PM<sub>2.5</sub>  
368 concentrations increased, with the largest increases of more than 20 µg m<sup>-3</sup>  
369 in the North China Plain and Eastern China, 10 µg m<sup>-3</sup> maximum increase  
370 in the Southwestern China and 5 µg m<sup>-3</sup> in the Northeastern, Southern and  
371 Central-West China, during the most polluted days compared to the normal  
372 days.

373 The increase in near-surface PM<sub>2.5</sub> concentrations during the most  
374 polluted day over Northeastern China is largely influenced by the local  
375 emissions, which contribute to a regional averaged concentration increase  
376 of 1.1 µg m<sup>-3</sup>. This is mainly due to the accumulation of local aerosols  
377 under the weakened prevailing northwesterly winds over this region.

378 When the PM<sub>2.5</sub> pollution occurred in the North China Plain, [on](#)  
379 [February 11, 2020, which was also reported as the polluted day in](#)

380 [observations \(Huang et al., 2020\)](#), the concentration of PM<sub>2.5</sub> was 16.1 μg  
381 m<sup>-3</sup> higher than that in normal days. The contribution from local emissions  
382 accounts for 66% of the averaged increase, which was related to the  
383 stagnant air condition (i.e., weakened lower tropospheric winds) resulting  
384 from the anomalous mid-tropospheric high pressure located at the  
385 climatological location of the East Asia trough (Fig. [S4S5](#)). Sources from  
386 Eastern China also explain 4.3 μg m<sup>-3</sup> (27%) of the total increase over the  
387 North China Plain.

388 During the most polluted day in Eastern China (the same day as the  
389 [most](#) polluted day in North China Plain), the ~~regional averaged increase in~~  
390 ~~concentration of~~ PM<sub>2.5</sub> ~~concentrations is was~~ 16 μg m<sup>-3</sup> [higher than that in](#)  
391 [normal days](#), which is primarily contributed by the local emissions. While  
392 the contribution from the North China Plain decreased in the [most](#) polluted  
393 day, the anomalous southerly winds brought more aerosols from Southern  
394 China and ROW into Eastern China, contributing to 4% and 10% aerosol  
395 increase, respectively.

396 Owing to the enhanced northerly winds, emissions from the North  
397 China Plain and Eastern China contribute 33% and 39% of the increase,  
398 respectively, in PM<sub>2.5</sub> concentration over Southern China. The most  
399 polluted day in Central-West China is mostly caused by local emissions  
400 (65% of the total increase).

401 When Southwestern China was under the polluted condition, PM<sub>2.5</sub>



402 concentration ~~was~~ increased by  $2.1 \mu\text{g m}^{-3}$ . Emissions from ROW,  
403 especially those from South and Southeast Asia, are of great significance  
404 to the increase of  $\text{PM}_{2.5}$  concentrations due to the enhanced southwesterly  
405 winds over this region. The relative contribution from ROW emissions is  
406 more than 50% over Southwestern China during the most polluted day. It  
407 highlights that the important role of transboundary transport needs to be  
408 considered when controlling local emissions to improve air quality in the  
409 near future.

410

## 411 **6. Conclusions and discussions**

412 The COVID-19 pandemic disrupted human activities and lead to abrupt  
413 reductions in anthropogenic emissions. This study first investigated the  
414 source contributions to  $\text{PM}_{2.5}$  over various regions covering the whole  
415 China during the COVID-19 pandemic. We pay attention not only to local  
416 emissions, but also to the impacts from regional and foreign transport of  
417 aerosols. An explicit aerosol source tagging is implemented in the  
418 Community Atmosphere Model version 5 (CAM5-EAST) to examine the  
419 aerosol transport pathways and source attribution of  $\text{PM}_{2.5}$  in China during  
420 the first few weeks of the COVID-19 outbreak (Week 1: January 30–  
421 February 5, Week 2: February 6–February 12 and Week 3: February 13–  
422 February 19). The contributions of emissions to  $\text{PM}_{2.5}$  originating from  
423 eight source regions in the mainland of China, including Northeastern

424 China, North China Plain, Eastern China, Southern China, Central-West  
425 China, Southwestern China, Northwestern China and Himalayas and  
426 Tibetan Plateau, and sources outside China (ROW) to near-surface  
427 concentrations, column burdens, transport pathways of PM<sub>2.5</sub>, and haze  
428 formation in different receptor regions in China are quantified in this study.

429 Aerosols emitted from the North China Plain, where the air quality is  
430 often poor, can be transported through Eastern China and reach  
431 Southwestern China during the three time periods. Similarly, aerosols from  
432 Eastern China move straight to Southern China and Southwestern China  
433 during Week 1 and Week 2, and a significant portion can also enter the  
434 North China Plain during Week 2 and Week 3.

435 Across the southern boundary of the mainland of China, high  
436 concentrations of PM<sub>2.5</sub> from South and Southeast Asia are lifted into the  
437 free atmosphere and then transported to Southern and Southwestern China.  
438 While PM<sub>2.5</sub> from the North China Plain and Eastern China can also be  
439 brought out of China via westerly winds, mostly below 700 hPa.

440 PM<sub>2.5</sub> in China is affected not only by local emissions but also by long-  
441 range transport of pollutants from distant source regions. Over the North  
442 China Plain, 40–66% of the PM<sub>2.5</sub> burden is attributed to local emissions  
443 during the COVID-19 outbreak. They also impact PM<sub>2.5</sub> in neighboring  
444 regions, accounting for 14–33% of the PM<sub>2.5</sub> burden in Eastern China and  
445 7–23% in Southern China during the three time periods. Northeastern

446 China has 36%-43% of local source contributions to its PM<sub>2.5</sub> column  
447 burden, while 39%-54% is contributed by emissions from ROW during the  
448 three time periods. In Eastern China, local emissions explain 27–40% of  
449 PM<sub>2.5</sub> burden, while ROW contributes 20–45%. In Southwestern China,  
450 59–78% of the PM<sub>2.5</sub> burden is contributed by emissions from ROW. Over  
451 the Northwestern China and Himalayas and Tibetan Plateau, ROW  
452 emissions have a great contribution of more than 70% to the PM<sub>2.5</sub> column  
453 burden.

454 In this study, the most polluted day is defined as the day with the  
455 highest daily PM<sub>2.5</sub> concentration in February 2020 for each receptor  
456 region in China. The transport from outside of China only has a great  
457 impact on some specific regions in China. In Southwestern China, the  
458 relative contribution from ROW emissions, especially those from South  
459 and Southeast Asia, to the increment of PM<sub>2.5</sub> concentration during the  
460 most polluted days compared with normal days is more than 50%. It is  
461 consistent with the previous studies that emissions from South and  
462 Southeast Asia have an important impact on air quality in southwest China  
463 (Yang et al., 2017a; Zhu et al., 2016, 2017). For other receptor regions in  
464 China (Northeastern China, North China Plain, Eastern China, Southern  
465 China and Central-West China), PM<sub>2.5</sub> concentrations are largely  
466 contributed by local emissions during the most polluted days compared  
467 with normal days. In the future with emissions reductions for better air

[quality in China, decreasing air pollution should consider aerosols from both Chinese local emissions and pollutant transport from outside of China.](#)

Despite the large reductions in emissions, near-surface PM<sub>2.5</sub> concentrations in the North China Plain and Eastern China increased a lot during the most polluted days of COVID-19 lockdown (with the highest daily PM<sub>2.5</sub> concentration in February 2020), with the largest increases of more than 20 µg m<sup>-3</sup>. In addition to local emissions, regional transport of pollutants is also an important factor that causes haze events in China. The increases in PM<sub>2.5</sub> concentrations during the most polluted days over the North China Plain and Eastern China are largely influenced by the stagnant air condition resulting from the anomalous high pressure system and weakening of winds, which lead to a reduced ventilation and aerosol accumulation in the North China Plain, together with an increase in aerosol inflow from regional transport. During the most polluted day in Southwestern China, ROW contributes over 50% of the PM<sub>2.5</sub> concentration increase, with enhanced southwesterly winds that drive pollution transport from South and Southeast Asia. It indicates that regional transport and unfavorable meteorology need to be taken into consideration when controlling local emissions to improve air quality in the near future.

[To highlight the roles of regional and foreign transport, the differences between Covid and Baseline simulations in relative contributions to PM<sub>2.5</sub> burden from local, region \(RCN\) and foreign \(ROW\) emissions are given](#)

490 in Figure S6. During the COVID-19 period, the local and RCN emission  
491 contributions to PM<sub>2.5</sub> were 1–4% lower than that in Base experiment over  
492 NCP and NEC. In Eastern China, the contribution from the local emissions  
493 decreased by 3–4% compared with Base experiment, while the  
494 contribution from ROW increased by more than 5%. In Southern China,  
495 50–70% of the PM<sub>2.5</sub> burden is contributed by emissions from ROW in  
496 Base experiment. During the COVID-19 period with low emission levels,  
497 the contribution from ROW to PM<sub>2.5</sub> burden in Southern China had an  
498 increase of more than 5%. It indicates that the important role of  
499 transboundary transport needs to be considered when controlling local  
500 emissions to improve air quality in the near future.

501 Many studies have examined the importance of meteorology on  
502 regional air quality during the COVID-19 lockdown period and  
503 emphasized that, when meteorology is unfavorable, abrupt emissions  
504 reductions cannot avoid severe air pollutions (Le et al. 2020; Sulaymon et  
505 al. 2021; Shen et al. 2021). Through model simulations, Le et al. (2020)  
506 found that abnormally high humidity promotes the heterogeneous  
507 chemistry of aerosols, which have contributed to the increase of PM<sub>2.5</sub> by  
508 12% in northern China during the city lockdown period. Sulaymon et al.  
509 (2021) found that significant increase in PM<sub>2.5</sub> concentrations caused by  
510 unfavorable meteorological conditions in Beijing-Tianjin-Hebei region  
511 during the lockdown period based on Community Multiscale Air Quality

512 (CMAQ) model simulations. By analyzing the observational data and  
513 model simulations, Shen et al. (2021) reported that 50% of the pollution  
514 episodes during the COVID-19 lockdown in Hubei of China were due to  
515 the stagnant meteorological conditions. Huang et al. (2020) found that the  
516 stagnant air conditions and enhanced atmospheric oxidizing capacity  
517 caused a severe haze event during the same time period. In line with  
518 previous studies, we also revealed the stagnant air condition under the  
519 anomalous high pressure system in the most polluted day over the North  
520 China Plain. In addition to the meteorological conditions, the effect of  
521 foreign transport was also raised in this study causing aerosol pollution in  
522 southwestern China during COVID-19 outbreak.

523 There are a few uncertainties in this study. The CAM5 model has low  
524 biases in reproducing the near-surface PM<sub>2.5</sub> concentrations in China,  
525 compared to observations, in part due to the incapability of simulating  
526 some aerosol components of PM<sub>2.5</sub> (e.g., ammonium and nitrate), excessive  
527 aerosol wet removal during the long-range transport (Wang et al., 2013),  
528 and uncertainties in observations. In majority of the climate models, the  
529 simulation of nitrate and ammonium aerosols are not included in the  
530 aerosol schemes, partly due to the complexity of calculation efficiency. For  
531 example, in many of the CMIP6 models, only two of them provide nitrate  
532 and ammonium mass mixing ratios. Many previous studies have evaluated  
533 the global climate models performance in reproducing aerosol

534 [concentrations \(e.g., Fan et al., 2018; Shindell et al., 2013; Yang et al.,](#)  
535 [2017a,b\). In general, the models can well simulate aerosols in North](#)  
536 [America and Europe but significantly underestimates aerosols in East Asia](#)  
537 [by about -36 to -58 % compared with observations. It can lead to an](#)  
538 [underestimation of aerosols contributed by Chinese local emissions in](#)  
539 [magnitudes, but might not change the main conclusions of this study.](#)

540 Uncertainties in the estimate of emission reductions in different source  
541 regions during the COVID-19 pandemic can also introduce uncertainties  
542 to our results. During the COVID-19 lockdown, greenhouse gas emissions  
543 also decreased (Le Quéré et al., 2020), but the effect of greenhouse gas  
544 reduction on meteorology that potentially influence aerosol distributions  
545 was not taken into consideration. Nevertheless, this study is the first  
546 attempt to provide source apportionment of aerosols [in covering the whole](#)  
547 China during the COVID-19 outbreak, which is beneficial to the  
548 investigation of policy implications for future air pollution control.

549 ***Data availability.***

550 The CAM5 model is available at  
551 <http://www.cesm.ucar.edu/models/cesm1.2/> (last access: ~~25 October 2020~~  
552 [August 2021](#)). CAM5-EAST model code and results can be made available  
553 upon request. The surface PM<sub>2.5</sub> observations are from the China National  
554 Environmental Monitoring Center (CNEMC, <http://www.cnemc.cn>, last  
555 access: ~~25 October 2020~~ [August 2021](#))

556 ***Competing interests.***

557 The authors declare that they have no conflict of interest.

558 ***Author contribution.***

559 YY and LR designed the research; YY performed the model simulations;  
560 LR analyzed the data. All authors discussed the results and wrote the paper.

561 ***Acknowledgments.***

562 This study was supported by the National Key Research and Development  
563 Program of China (grant 2020YFA0607803 [and 2019YFA0606800](#)) and  
564 the National Natural Science Foundation of China (grant 41975159). HW  
565 acknowledges the support by the U.S. Department of Energy (DOE),  
566 Office of Science, Office of Biological and Environmental Research (BER).  
567 The Pacific Northwest National Laboratory (PNNL) is operated for DOE  
568 by the Battelle Memorial Institute under contract DE-AC05-76RLO1830.



569

## Reference

570

571 Anderson, T.L., Charlson, R.J., Schwartz, S.E., Knutti, R., Boucher, O., Rodhe, H., Heintzenberg,  
572 J.: Climate forcing by aerosol—a hazy picture, *Science*, 300, 1103–1104,  
573 <https://doi.org/10.1126/science.1084777>, 2003.

574

575 Bao, R., Zhang, A.: Does lockdown reduce air pollution? Evidence from 44 cities in northern China,  
576 ~~Science~~ ~~of~~ ~~The~~ ~~Total~~ ~~Environment~~ ~~Environ.~~, 731, 139052,  
577 <https://doi.org/10.1016/j.scitotenv.2020.139052>, 2020.

578

579 Chai, F., Gao, J., Chen, Z., Wang, S., Zhang, Y., Zhang, J., Zhang, H., Yun, Y., Ren, C.: Spatial and  
580 temporal variation of particulate matter and gaseous pollutants in 26 cities in China, ~~Journal of~~  
581 ~~Environmental—Environ. Sciences~~ ~~Sci.~~, 26, 75–82, [https://doi.org/10.1016/S1001-](https://doi.org/10.1016/S1001-0742(13)60383-6)  
582 [0742\(13\)60383-6](https://doi.org/10.1016/S1001-0742(13)60383-6), 2014.

583

584 China State Council: Action Plan on Prevention and Control of Air Pollution, China State Council,  
585 Beijing, China, [http://www.gov.cn/zwggk/2013-09/12/content\\_2486773.htm](http://www.gov.cn/zwggk/2013-09/12/content_2486773.htm) (last access: 27  
586 September 2020), 2013.

587

588 Dong, E., Du, H., Gardner, L.: An interactive web-based dashboard to track COVID-19 in real time,  
589 ~~Lancet Infectious—Infect. Diseases~~ ~~Dis.~~, 20, 533–534, [https://doi.org/10.1016/S1473-](https://doi.org/10.1016/S1473-3099(20)30120-1)  
590 [3099\(20\)30120-1](https://doi.org/10.1016/S1473-3099(20)30120-1), 2020.

591

592 Fan, H., Zhao, C., Yang, Y.: A comprehensive analysis of the spatio-temporal variation of urban air  
593 pollution in China during 2014–2018, ~~Atmos. Environ.~~ ~~Atmospheric Environment~~, 220,  
594 117066, <https://doi.org/10.1016/j.atmosenv.2019.117066>, 2020.

595

596 [Fan, T., Liu, X., Ma, P.-L., Zhang, Q., Li, Z., Jiang, Y., Zhang, F., Zhao, C., Yang, X., Wu, F., and](#)  
597 [Wang, Y.: Emission or atmospheric processes? An attempt to attribute the source of large bias](#)  
598 [of aerosols in eastern China simulated by global climate models, \*Atmos. Chem. Phys.\*, 18,](#)  
599 [1395–1417, <https://doi.org/10.5194/acp-18-1395-2018>, 2018.](#)

600

601 Gelaro, R., McCarty, W., Suárez, M. J., Todling, R., Molod, A., Takacs, L., Randles, C. A.,  
602 Darmenov, A., Bosilovich, M. G., Reichle, R., Wargan, K., Coy, L., Cullather, R., Draper, C.,  
603 Akella, S., Buchard, V., Conaty, A., da Silva, A. M., Gu, W., Kim, G., Koster, R., Lucchesi, R.,  
604 Merkova, D., Nielsen, J. E., Partyka, G., Pawson, S., Putman, W., Rienecker, M., Schubert, S.  
605 D., Sienkiewicz, M., Zhao, B.: The Modern-Era Retrospective Analysis for Research and  
606 Applications, Version 2 (MERRA-2), *J. Climate*, 30, 5419–5454, [https://doi.org/10.1175/JCLI-](https://doi.org/10.1175/JCLI-D-16-0758.1)  
607 [D-16-0758.1](https://doi.org/10.1175/JCLI-D-16-0758.1), 2017.

608

609 Hadley, O. L., Ramanathan, V., Carmichael, G. R., Tang, Y., Corrigan, C. E., Roberts, G. C., Mauger,  
610 G. S.: Trans-Pacific transport of black carbon and fine aerosol ( $D < 2.5\mu\text{m}$ ) into North America,  
611 ~~J. Geophys. Res.~~ ~~Journal of Geophysical Research~~, 112, D05309,

612 <https://doi.org/10.1029/2006JD007632>, 2007.

613

614 Heft-Neal, S., Burney, J., Bendavid, E., Burke, M.: Robust relationship between air quality and  
615 infant mortality in Africa, *Nature*, 559, 254. <https://doi.org/10.1038/s41586-018-0263-3>, 2018.

616

617 Hurrell, J. W., Holland, M. M., Gent, P. R., Ghan, S., Kay, J. E., Kushner, P. J., Lamarque, J. F.,  
618 Large, W. G., Lawrence, D., Lindsay, K., Lipscomb, W. H., Long, M. C., Mahowald, N.,  
619 Marsh, D. R., Neale, R. B., Rasch, P., Vavrus, S., Vertenstein, M., Bader, D., Collins, W. D.,  
620 Hack, J. J., Kiehl, J., Marshall, S.: The Community Earth System Model A Framework for  
621 Collaborative Research, *Bulletin Of The American Meteorological Society*,  
622 94, 1339–1360, <https://doi.org/10.1175/BAMS-D-12-00121.1>, 2013.

623

624 Huang, X., Ding, A., Gao, J., Zheng, B., Zhou, D., Qi, X., Tang, R., Ren, C., Nie, W., Chi, X., Wang,  
625 J., Xu, Z., Chen, L., Li, Y., Che, F., Pang, N., Wang, H., Tong, D., Qin, W., Cheng, W., Liu, W.,  
626 Fu, Q., Chai, F., Davis, S. J., Zhang, Q., He, K.: Enhanced secondary pollution offset reduction  
627 of primary emissions during COVID-19 lockdown in China, *National Science  
628 Review*, nwaal37, <https://doi.org/10.1093/nsr/nwaa137>, 2020.

629

630 Kong, L., Feng, M., Liu, Y., Zhang, Y., Zhang, C., Li, C., Qu, Y., An, J., Liu, X., Tan, Q., Cheng, N.,  
631 Deng, Y., Zhai, R., Wang, Z.: Elucidating the pollution characteristics of nitrate, sulfate and  
632 ammonium in PM<sub>2.5</sub> in Chengdu, southwest China, based on 3-year measurements, *Atmos.  
633 Chem. Phys., Atmospheric Chemistry and Physics*, 20, 11181–11199,  
634 <https://doi.org/10.5194/acp-20-11181-2020>, 2020.

635

636 Liao, H., Chang, W., Yang, Y.: Climatic effects of air pollutants over China: A review, *Advances in  
637 Atmospheric Sciences*, 32, 115–139, <https://doi.org/10.1007/s00376-014-0013-x>,  
638 2015.

639

640 Le, T., Wang, Y., Liu, L., Yang, J., Yung, Y. L., Li, G., Seinfeld, J. H.: Unexpected air pollution with  
641 marked emission reductions during the COVID-19 outbreak in China, *Science*, 369, 702–706,  
642 <https://doi.org/10.1126/science.abb7431>, 2020.

643

644 Le Quéré, C., Jackson, R. B., Jones, M. W., Smith, A. J. P., Abernethy, S., Andrew, R. M., De-Gol,  
645 A. J., Willis, D. R., Shan, Y. L., Canadell, J. G., Friedlingstein, P., Felix Creutzig, F., Peters,  
646 G., P.: Temporary reduction in daily global CO<sub>2</sub> emissions during the COVID-19 forced  
647 confinement, *Nature Climate Change*, 10, 647–653,  
648 <https://doi.org/10.1038/s41558-020-0797-x>, 2020.

649

650 Lelieveld, J., Klingmüller, K., Pozzer, A., Burnett, R. T., Haines, A., Ramanathan, V.: Effects of fossil  
651 fuel and total anthropogenic emission removal on public health and climate. *P. Natl. Acad.  
652 Sci. Proceedings of the National Academy of Sciences*, 116, 7192–7197,  
653 <https://doi.org/10.1073/pnas.1819989116>, 2019.

654

655 Li, L., Li, Q., Huang, L., Wang, Q., Zhu, A., Xu, J., Liu, Z., Li, H., Shi, L., Li, R., Azari, M., Wang,

656 Y., Zhang, X., Liu, Z., Zhu, Y., Zhang, K., Xue, S., Ooi, M., C., G., Zhang, D., Chan, A.: Air  
657 quality changes during the COVID-19 lockdown over the Yangtze River Delta Region: An  
658 insight into the impact of human activity pattern changes on air pollution variation. *Science of  
659 The Total Environment Environ.*, 732, 139282. <https://doi.org/10.1016/j.scitotenv.2020.139282>,  
660 2020.

661

662 Liu, X., Easter, R. C., Ghan, S. J., Zaveri, R., Rasch, P., Shi, X., Lamarque, J., F., Gettelman, A.,  
663 Morrison, H., Vitt, F., Conley, A., Park, S., Neale, R., Hannay, C., Ekman, A. M. L., Hess, P.,  
664 Mahowald, N., Collins, W., Iacono, M. J., Bretherton, C. S., Flanner, M. G., Mitchell, D.:  
665 Toward a minimal representation of aerosols in climate models: description and evaluation in  
666 the Community Atmosphere Model CAM5, *Geoscientific Geosci. Model Development Dev.*, 5,  
667 709–739. <https://doi.org/10.5194/gmd-5-709-2012>, 2012.

668

669 Liu, Y., Hong, Y., Fan, Q., Wang, X., Chan, P., Chen, X., Lai, A., Wang, M., Chen, X.: Source-  
670 receptor relationships for PM<sub>2.5</sub> during typical pollution episodes in the Pearl River Delta city  
671 cluster, China, *Science of The Total Environment Environ.*, 596, 194-206,  
672 <https://doi.org/10.1016/j.scitotenv.2017.03.255>, 2017.

673

674 [Lund, M. T., Myhre, G., and Samset, B. H.: Anthropogenic aerosol forcing under the Shared  
675 Socioeconomic Pathways, \*Atmos. Chem. Phys.\*, 19, 13827–13839,  
676 <https://doi.org/10.5194/acp-19-13827-2019>, 2019.](#)

677

678 [Lyakaremye, V., Zeng, G., Siebert, A., Yang, X.: Contribution of external forcings to the observed  
679 trend in surface temperature over Africa during 1901–2014 and its future projection from  
680 CMIP6 simulations, \*Atmos. Res.\*, 254, 105512,  
681 <https://doi.org/10.1016/j.atmosres.2021.105512>, 2021.](#)

682

683 Ramanathan, V. C. P. J., Crutzen, P. J., Kiehl, J. T., Rosenfeld, D.: Aerosols, climate, and the  
684 hydrological cycle, *science*, 294, 2119-2124, <https://doi.org/10.1126/science.1064034>, 2001.

685

686 Ren, L., Yang, Y., Wang, H., Zhang, R., Wang, P., Liao, H.: Source attribution of Arctic aerosols and  
687 associated Arctic warming trend during 1980–2018, *Atmos. Chem. Phys., Atmospheric  
688 Chemistry and Physics*, 20, 9067-9085, <https://doi.org/10.5194/acp-2020-3,2020>.

689

690 Sharma, S., Zhang, M., Anshika, Gao, J., Kota, S. H.: Effect of restricted emissions during covid-  
691 19 on air quality in india, *Science of The Total Environment Environ.*, 728, 138878,  
692 <https://doi.org/10.1016/j.scitotenv.2020.138878>, 2020.

693

694 [Shen, L., Zhao, T., Wang, H., Liu, J., Bai, Y., Kong, S., Zheng, H., Zhu, Y., Shu, Z.: Importance of  
695 meteorology in air pollution events during the city lockdown for COVID-19 in Hubei Province,  
696 Central China, \*Sci. Total Environ.\*, 754, 142227,  
697 <https://doi.org/10.1016/j.scitotenv.2020.142227>, 2021.](#)

698

699 [Shindell, D. T., Lamarque, J.-F., Schulz, M., Flanner, M., Jiao, C., Chin, M., Young, P. J., Lee, Y.](#)

700 [H., Rotstayn, L., Mahowald, N., Milly, G., Faluvegi, G., Balkanski, Y., Collins, W. J., Conley,](#)  
701 [A. J., Dalsoren, S., Easter, R., Ghan, S., Horowitz, L., Liu, X., Myhre, G., Nagashima, T., Naik,](#)  
702 [V., Rumbold, S. T., Skeie, R., Sudo, K., Szopa, S., Takemura, T., Voulgarakis, A., Yoon, J.-H.,](#)  
703 [and Lo, F.: Radiative forcing in the ACCMIP historical and future climate simulations, \*Atmos.\*](#)  
704 [\*Chem. Phys.\*, 13, 2939–2974, <https://doi.org/10.5194/acp-13-2939-2013>, 2013.](#)  
705  
706 Smith, C. J., Kramer, R. J., Myhre, G., Alterskjær, K., Collins, W., Sima, A., Boucher, O., Dufresne,  
707 J.-L., Nabat, P., Michou, M., Yukimoto, S., Cole, J., Paynter, D., Shiogama, H., O'Connor, F.  
708 M., Robertson, E., Wiltshire, A., Andrews, T., Hannay, C., Miller, R., Nazarenko, L., Kirkevåg,  
709 A., Olivie, D., Fiedler, S., Lewinschal, A., Mackallah, C., Dix, M., Pincus, R., Forster, P. M.:  
710 Effective radiative forcing and adjustments in CMIP6 models, [Atmos. Chem.](#)  
711 [Phys., Atmospheric Chemistry and Physics](#), 20, 9591–9618, [https://doi.org/10.5194/acp-20-](https://doi.org/10.5194/acp-20-9591-2020)  
712 [9591-2020](https://doi.org/10.5194/acp-20-9591-2020), 2020.  
713  
714 [Sulaymon, I. D., Zhang, Y., Hopke, P. K., Hu, J., Zhang, Y., Li, L., Mei, X., Gong, K., Shi, Z., Zhao,](#)  
715 [B., Zhao, F.: Persistent high PM<sub>2.5</sub> pollution driven by unfavorable meteorological conditions](#)  
716 [during the COVID-19 lockdown period in the Beijing-Tianjin-Hebei region, China, \*Environ.\*](#)  
717 [Res., 198, 111186, <https://doi.org/10.1016/j.envres.2021.111186>, 2021.  
718  
719 Tian, H., Liu, Y., Li, Y., Wu, C., Chen, B., Kraemer, M.U.G., Li, B., Cai, J., Xu, B., Yang, Q., Wang,  
720 B., Yang, P., Cui, Y., Song, Y., Zheng, P., Wang, Q., Bjornstad, O.N., Yang, R., Grenfell, B.T.,  
721 Pybus, O.G., Dye, C.: An investigation of transmission control measures during the first 50  
722 days of the COVID-19 epidemic in China, \*Science\*, b6105  
723 <https://doi.org/10.1126/science.abb6105>, 2020.  
724  
725 Vautard, R., Yiou, P., Oldenborgh, G.: Decline of fog, mist and haze in Europe over the past 30 years,  
726 \[Nature Nat. Geoscience Geosci.\]\(#\), 2, 115–119, <https://doi.org/10.1038/ngeo414>, 2009.  
727  
728 Wang, H., Easter, R. C., Rasch, P. J., Wang, M., Liu, X., Ghan, S. J., Qian, Y., Yoon, J.-H., Ma, P.-  
729 L., Vinoj, V.: Sensitivity of remote aerosol distributions to representation of cloud–aerosol  
730 interactions in a global climate model, \[Geoscientific Geosci. Model Development Dev.\]\(#\), 6, 765–  
731 782, <https://doi.org/10.5194/gmd-6-765-2013>, 2013.  
732  
733 Wang, H., Rasch, P. J., Easter, R. C., Singh, B., Zhang, R., Ma, P. L., Qian, Y., Ghan, S. J., Beagley,  
734 N.: Using an explicit emission tagging method in global modeling of source-receptor  
735 relationships for black carbon in the Arctic: Variations, sources, and transport pathways,  
736 \[Journal of Geophysical Research Res.\]\(#\), 119, 12888–12909,  
737 <https://doi.org/10.1002/2014JD022297>, 2014.  
738  
739 Wang, H., Easter, R. C., Zhang, R., Ma, P., Singh, B., Zhang, K., Ganguly, D., Rasch, P. J., Burrows,  
740 S. M., Ghan, S. J., Lou, S., Qian, Y., Yang, Y., Feng, Y., Flanner, M., Leung, L. R., Liu, X.,  
741 Shrivastava, M., Sun, J., Tang, Q., Xie, S., Yoon, J.: Aerosols in the E3SM Version 1: New  
742 Developments and Their Impacts on Radiative Forcing, \[Journal of Advances in Modeling\]\(#\)  
743 \[Model. Earth Systems Sy.\]\(#\), 12, 293, <https://doi.org/10.1029/2019MS001851>, 2020.](#)

744

745 Wang, P., Chen, K., Zhu, S., Wang, P., Zhang, H.: Severe air pollution events not avoided by reduced  
746 anthropogenic activities during COVID-19 outbreak, Resources-Resour. Conservation-Conserv.  
747 and RecyclingRecycl., 158, 104814, <https://doi.org/10.1016/j.resconrec.2020.104814>, 2020.

748

749 Wang, Q., Huang, R. J., Cao, J., Tie, X., Shen, Z., Zhao, S., Han, Y., Li, G., Li, Z., Ni, H., Zhou, Y.,  
750 Wang, M., Chen, Y., Zhou, Y.: Contribution of regional transport to the black carbon aerosol  
751 during winter haze period in Beijing, Atmospheric-Atmos. EnvironmentEnviron., 132,11-28,  
752 <https://doi.org/10.1016/j.atmosenv.2016.02.031>, 2016.

753

754 Watson, J. G.: Visibility: Science and regulation. Journal of the Air and Waste Management Manage.  
755 AssociationAssoc., 52, 628-713, <https://doi.org/10.1080/10473289.2002.10470813>, 2002.

756

757 Xu, Q., Wang, S., Jiang, J., Bhattarai, N., Li, X., Chang, X., Qiu, X., Zheng, M., Hua, Y., Hao, J.:  
758 Nitrate dominates the chemical composition of PM<sub>2.5</sub> during haze event in Beijing, China, The  
759 Science of the Total EnvironmentEnviron., 689, 1293–1303.  
760 <https://doi.org/10.1016/j.scitotenv.2019.06.294>, 2019.

761

762 Xue, W. B., Fu, F., Wang, J. N., Tang, G. Q., Lei, Y., Yang, J. T., Wang, Y. S.: Numerical study on  
763 the characteristics of regional transport of PM<sub>2.5</sub> in China, Journal of Environmental Environ.  
764 Sciences China, 34, 1361–1368, 2014.

765

766 Yang, Y., Wang, H., Smith, S. J., Ma, P. L., Rasch, P. J.: Source attribution of black carbon and its  
767 direct radiative forcing in China, Atmospheric Atmos. Chemistry and PhysiesPhys., 17, 4319–  
768 4336, <https://doi.org/10.5194/acp-17-4319-2017>, 2017a.

769

770 Yang, Y., Wang, H., Smith, S. J., Easter, R., Ma, P. L., Qian, Y., Yu, H., Li, C., Rasch, P. J.: Global  
771 source attribution of sulfate concentration and direct and indirect radiative forcing,  
772 Atmospheric Atmos. Chemistry and PhysiesPhys., 17, 8903–8922,  
773 <https://doi.org/10.5194/acp-17-8903-2017>, 2017b.

774

775 Yang, Y., Wang, H., Smith, S. J., Zhang, R., Lou, S., Qian, Y., Ma, P.-L., Rasch, P. J.: Recent  
776 intensification of winter haze in China linked to foreign emissions and meteorology, Sci.  
777 Rep.Scientific Reports, 8, 2107, <https://doi.org/10.1038/s41598-018-20437-7>, 2018a.

778

779 Yang, Y., Wang, H., Smith, S. J., Easter, R. C., Rasch, P. J.: Sulfate aerosol in the Arctic: Source  
780 attribution and radiative forcing, J. Geophys. Res.,Journal of Geophysical Research:  
781 Atmospheres, 123, 1899–1918, <https://doi.org/10.1002/2017JD027298>, 2018b.

782

783 Yang, Y., Wang, H., Smith, S. J., Zhang, R., Lou, S., Yu, H., Li, C., Rasch, P. J.: Source  
784 apportionments of aerosols and their direct radiative forcing and long-term trends over  
785 continental United States, Earth's Future, 6, 793–808, <https://doi.org/10.1029/2018EF000859>,  
786 2018c.

787

788 Yang, Y., Smith, S. J., Wang, H., Lou, S., Rasch, P. J.: Impact of anthropogenic emission injection  
789 height uncertainty on global sulfur dioxide and aerosol distribution, ~~J. Geophys. Res., Journal~~  
790 ~~of Geophysical Research: Atmospheres,~~ 124, 4812–4826,  
791 <https://doi.org/10.1029/2018JD030001>, 2019a.

792

793 Yang, Y., Smith, S. J., Wang, H., Mills, C. M., Rasch, P. J.: Variability, timescales, and nonlinearity  
794 in climate responses to black carbon emissions, ~~Atmospheric Atmos. Chemistry and~~  
795 ~~Physics Phys.~~, 19, 2405–2420, <https://doi.org/10.5194/acp-19-2405-2019>, 2019b.

796

797 Yang, Y., Lou, S., Wang, H., Wang, P., Liao, H.: Trends and source apportionment of aerosols in  
798 Europe during 1980–2018, ~~Atmospheric Atmos. Chemistry and Physics Phys.~~, 20, 2579–2590,  
799 <https://doi.org/10.5194/acp-20-2579-2020>, 2020.

800

801 Yu, H. B., Remer, L. A., Chin, M., Bian, H. S., Tan, Q., Yuan, T. L., Zhang, Y.: Aerosols from  
802 overseas rival domestic emissions over North America, *Science*, 337, 566–569,  
803 <https://doi.org/10.1126/science.1217576>, 2012.

804

805 Yu, H., Remer, L. A., Chin, M., Bian, H., Kleidman, R. G., Diehl, T.: A satellite-based assessment  
806 of transpacific transport of pollution aerosol, ~~J. Geophys. Res., Journal of Geophysical~~  
807 ~~Research,~~ 113, D14S12, <https://doi.org/10.1029/2007JD009349>, 2008.

808

809 Zhang, R., Wang, H., Hegg, D. A., Qian, Y., Doherty, S. J., Dang, C., Ma, P. L., Rasch, P. J., Fu, Q.:  
810 Quantifying sources of black carbon in western North America using observationally based  
811 analysis and an emission tagging technique in the Community Atmosphere Model,  
812 ~~Atmospheric Atmos. Chemistry and Physics Phys.~~, 15, 12,805–12,822,  
813 <https://doi.org/10.5194/acpd-15-12957-2015>, 2015.

814

815 Zheng, B., Tong, D., Li, M., Liu, F., Hong, C., Geng, G., Li, H., Li, X., Peng, L., Qi, J., Yan, L.,  
816 Zhang, Y., Zhao, H., Zheng, Y., He, K., Zhang, Q.: Trends in China's anthropogenic emissions  
817 since 2010 as the consequence of clean air actions, ~~Atmospheric Atmos. Chemistry and~~  
818 ~~Physics Phys.s~~, 18, 14095–14111, <https://doi.org/10.5194/acp-18-14095-2018>, 2018.

819

820 [Zhuang, B. L., Li, S., Wang, T. J., Liu, J., Chen, H. M., Chen, P. L., Li, M. M., Xie, M.: Interaction](#)  
821 [between the Black Carbon Aerosol Warming Effect and East Asian Monsoon Using RegCM4,](#)  
822 [J. Climate, 31, 9367-9388, https://doi.org/10.1175/JCLI-D-17-0767.1, 2018.](#)

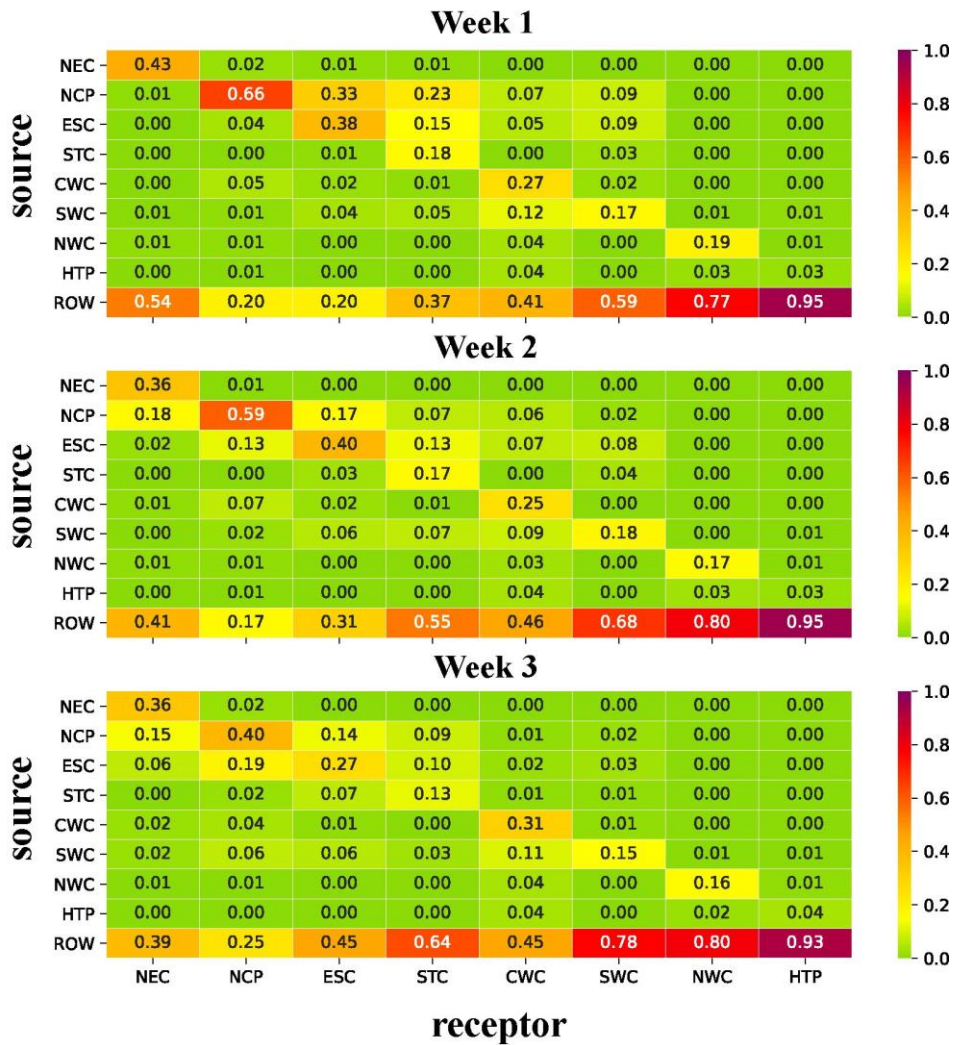
823

824 [Zhu, J., Xia, X., Che, H., Wang, J., Zhang, J., Duan, Y.: Study of aerosol optical properties at](#)  
825 [Kunming in southwest China and longrange transport of biomass burning aerosols from North](#)  
826 [Burma, Atmos. Res., 169, 237–247, https://doi.org/10.1016/j.atmosres.2015.10.012, 2016.](#)

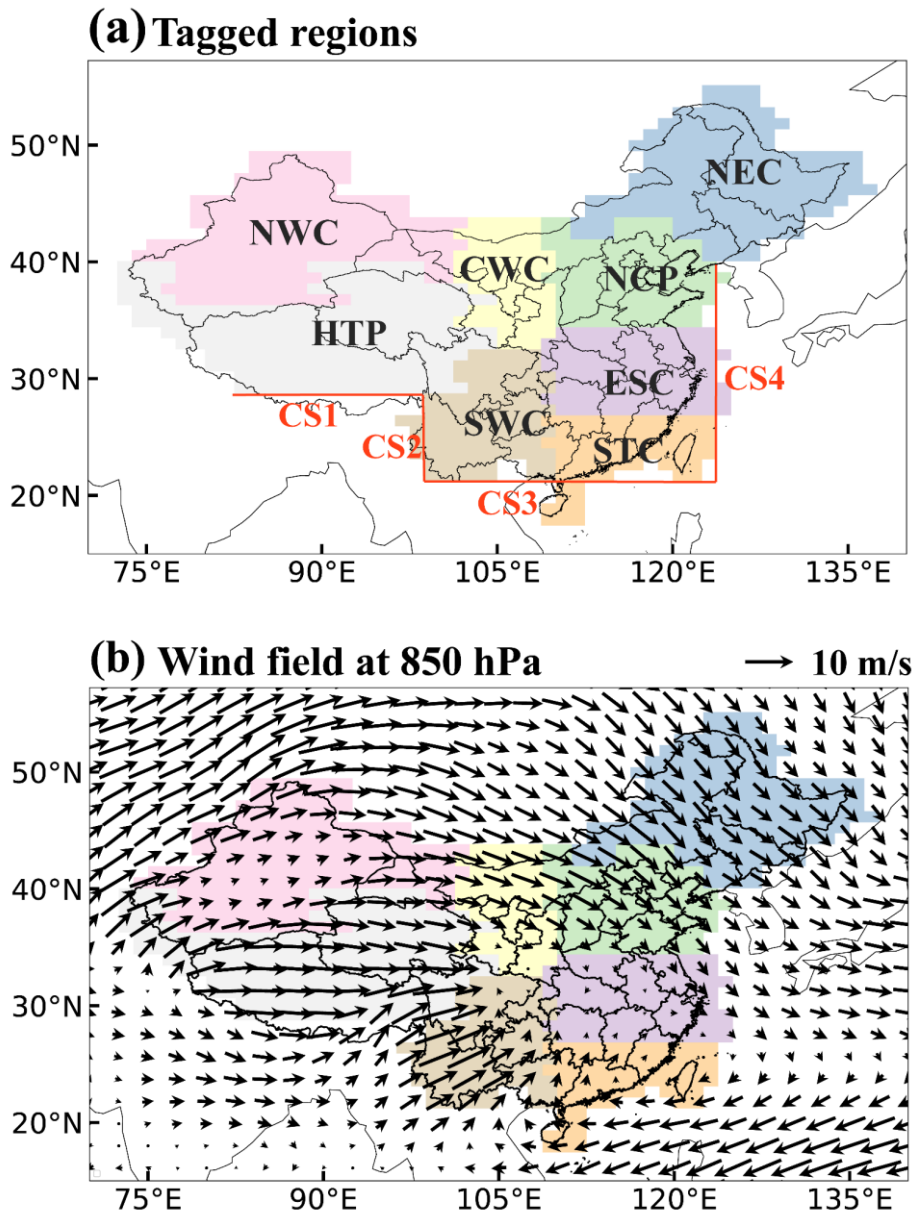
827

828 [Zhu, J., Xia, X., Wang, J., Zhang, J., Wiedinmyer, C., Fisher, J. A., Keller, C. A.: Impact of Southeast](#)  
829 [Asian smoke on aerosol properties in Southwest China: First comparison of model simulations](#)  
830 [with satellite and ground observations, J. Geophys. Res. Atmos., 122, 3904–3919,](#)  
831 [https://doi.org/10.1002/2016JD025793, 2017.](#)

832 **Table 1.** Fractional contributions of emissions from nine tagged source regions (vertical  
 833 axis) to mean PM<sub>2.5</sub> column burden in eight receptor regions (horizontal axis) during  
 834 the three time periods- ('Week 1': January 30–February 5, 'Week 2': February 6–  
 835 February 12 and 'Week 3': February 13–February 19).  
 836



837  
 838

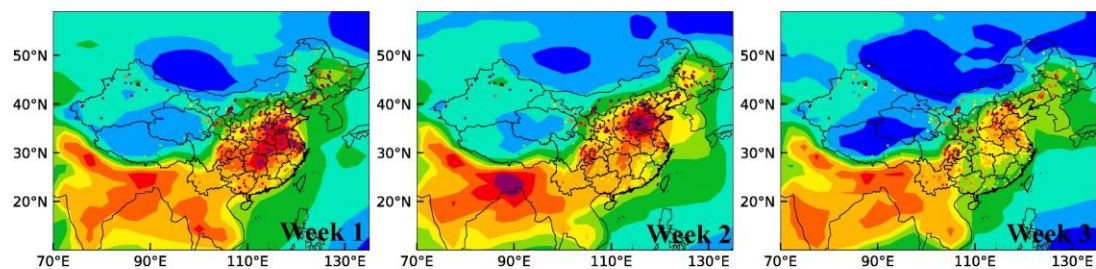


839  
 840  
 841  
 842  
 843  
 844  
 845  
 846  
 847  
 848  
 849  
 850

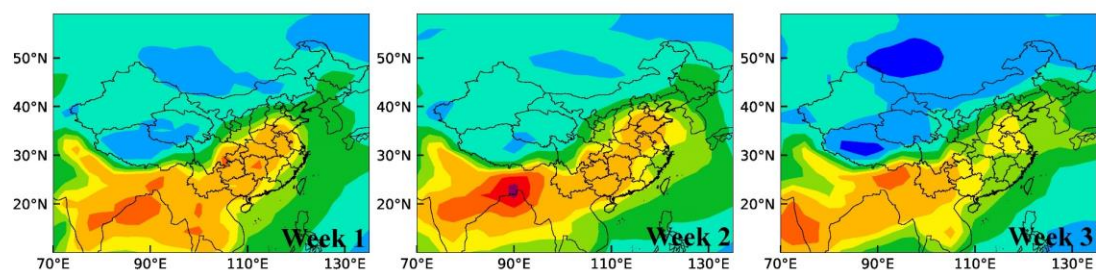
**Figure 1.** (a) Tagged source regions (NEC: Northeastern China, NCP: North China Plain, ESC: Eastern China, STC: Southern China, CWC: Central-West China, SWC: Southwestern China, NWC: Northwestern China, HTP: Himalayas and Tibetan Plateau, ROW: rest of the world) and (b) mean wind field (units:  $\text{m s}^{-1}$ , vectors) at 850 hPa during the [time period of interest: three weeks of the study from January 30 to February 19, which had the largest number of newly-diagnosed COVID-19 cases](#). Lines in (a) mark the cross-sections (CS) defined to study the transport of aerosols to and from China.



**(a) PM<sub>2.5</sub> surface conc. ( $\mu\text{g m}^{-3}$ )**



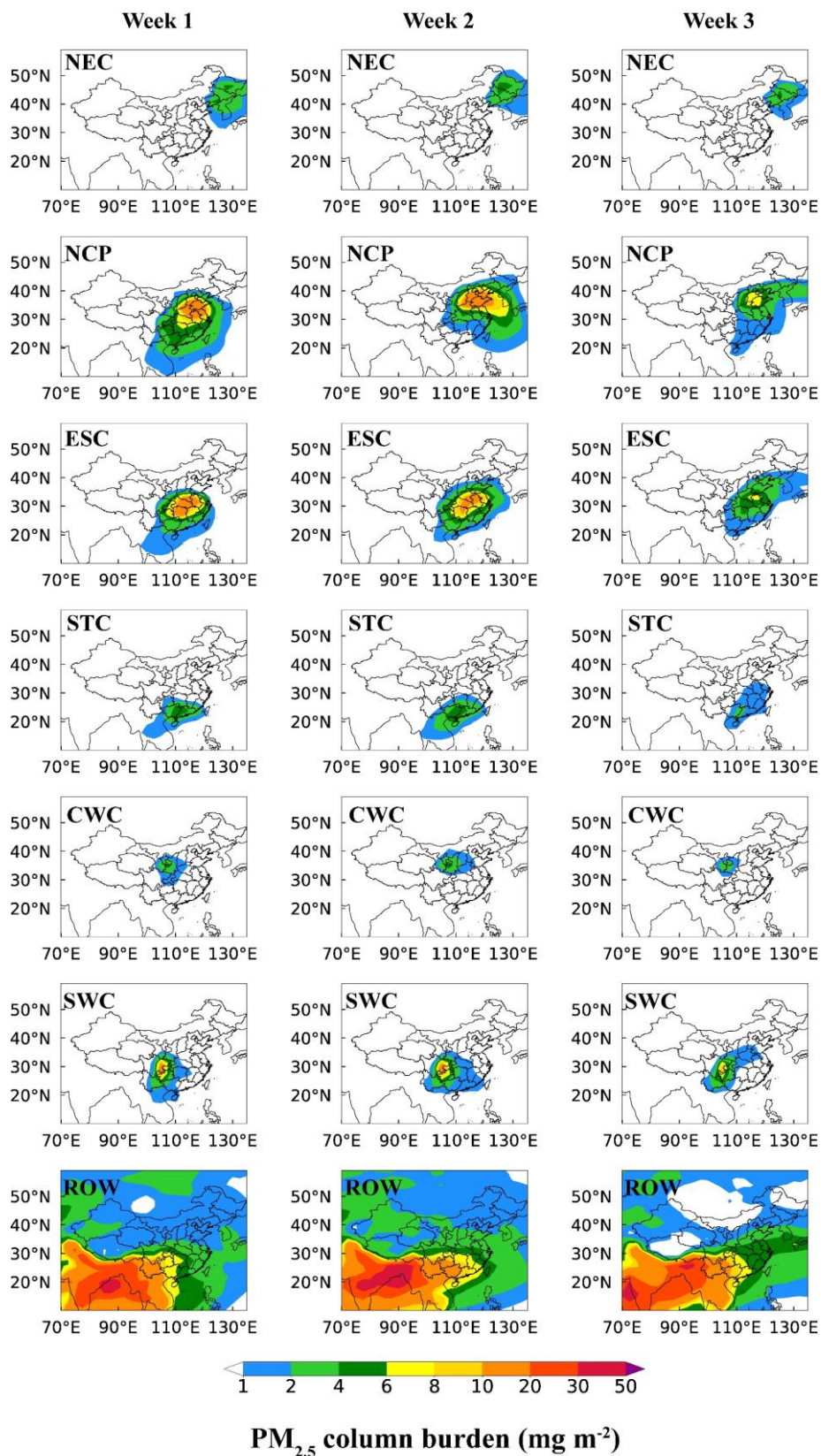
**(b) PM<sub>2.5</sub> column burden ( $\text{mg m}^{-2}$ )**



851

852

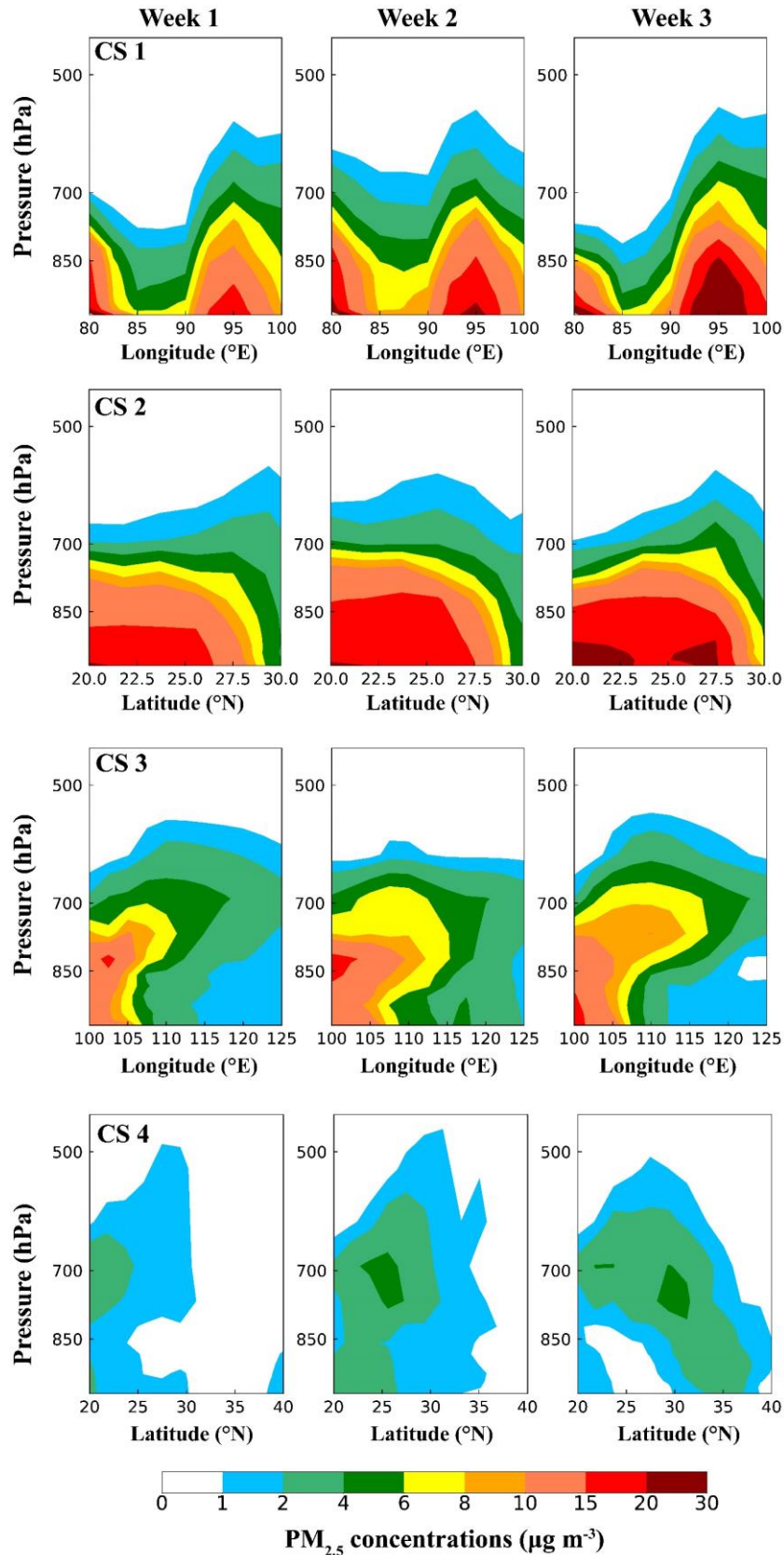
853 **Figure 2.** Spatial distribution of (a) the simulated and observed mean near-surface  
854 PM<sub>2.5</sub> concentrations ( $\mu\text{g m}^{-3}$ ) and (b) PM<sub>2.5</sub> column burden ( $\text{mg m}^{-2}$ ) during January  
855 30–February 5 (Week 1), February 6–February 12 (Week 2) and February 13–February  
856 19 (Week 3).



857

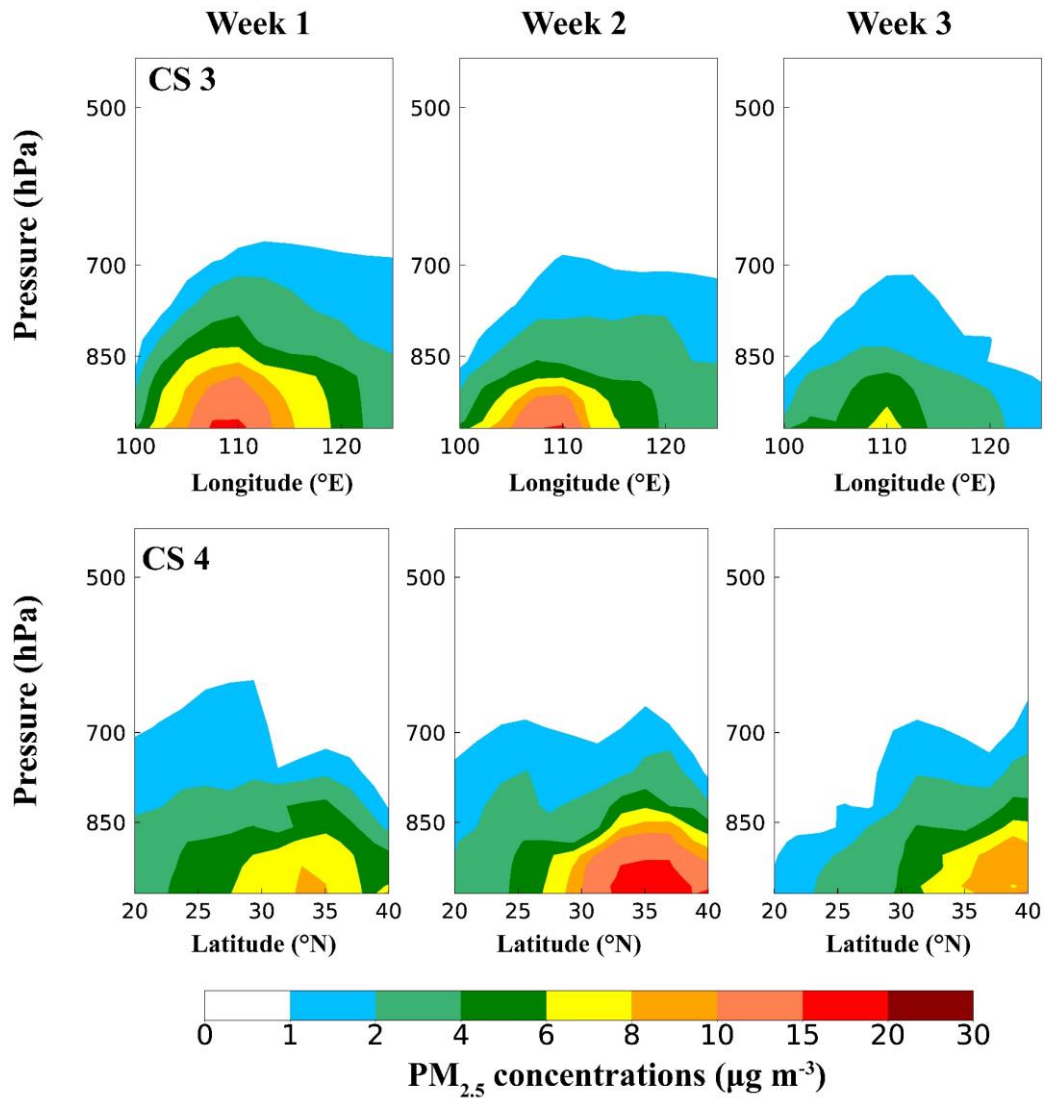
858 **Figure 43.** Spatial distribution of PM<sub>2.5</sub> column burden (mg m<sup>-2</sup>) originating from the  
 859 six major source regions in China (NEC, NCP, ESC, STC, CWC and SWC) and sources  
 860 outside China (ROW) during the three time periods.

861



862

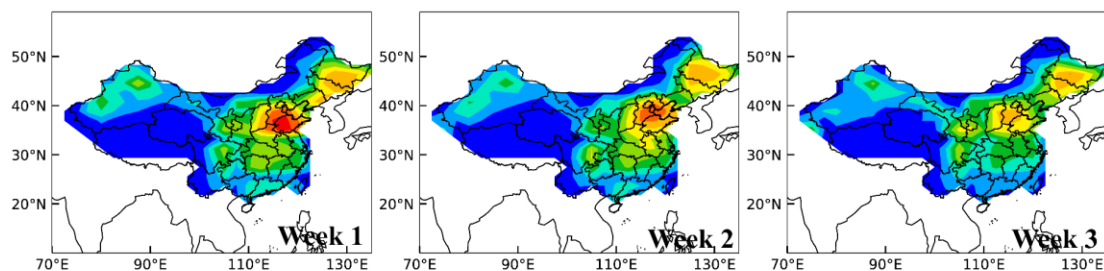
863 **Figure 54.** Vertical distributions of PM<sub>2.5</sub> concentrations (µg m<sup>-3</sup>), originating from  
 864 emissions outside China (i.e., ROW sources), across the latitudinal and/or longitudinal  
 865 extents marked in Fig.1, respectively, during the three time periods.



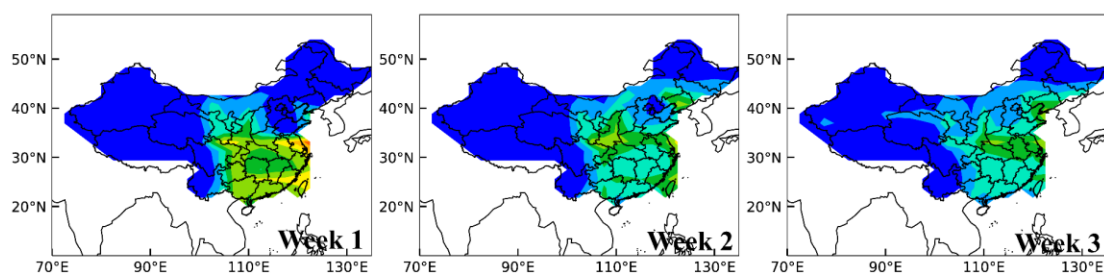
866  
 867  
 868  
 869  
 870  
 871  
 872  
 873

**Figure 65.** Vertical distributions of PM<sub>2.5</sub> concentrations (µg m<sup>-3</sup>), originating from domestic emissions in China, across the latitudinal and/or longitudinal extents marked in Fig.1, respectively, during the three time periods. The values along CS 1 and CS 2 are negligibly small.

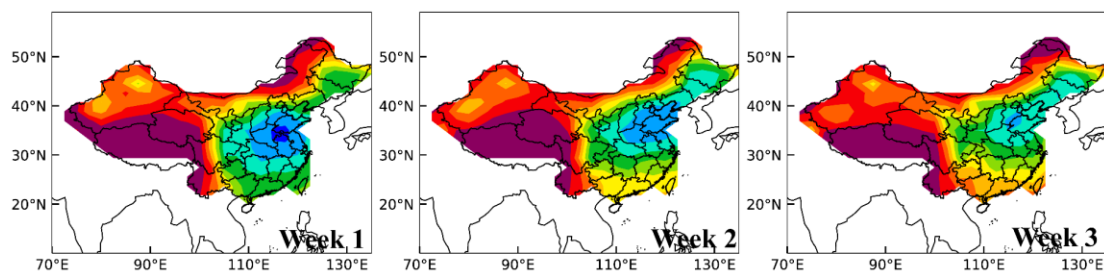
**(a) Local contribution**



**(b) RCN contribution**



**(c) ROW contribution**



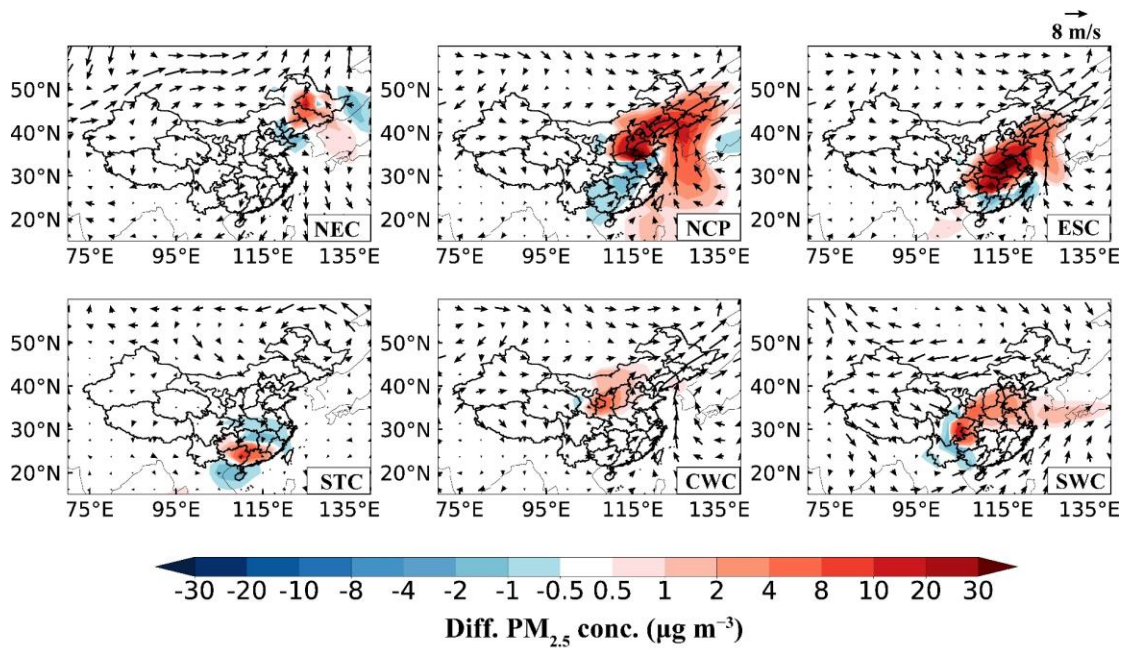
**Relative contribution to  $PM_{2.5}$  column burden (%)**

874

875

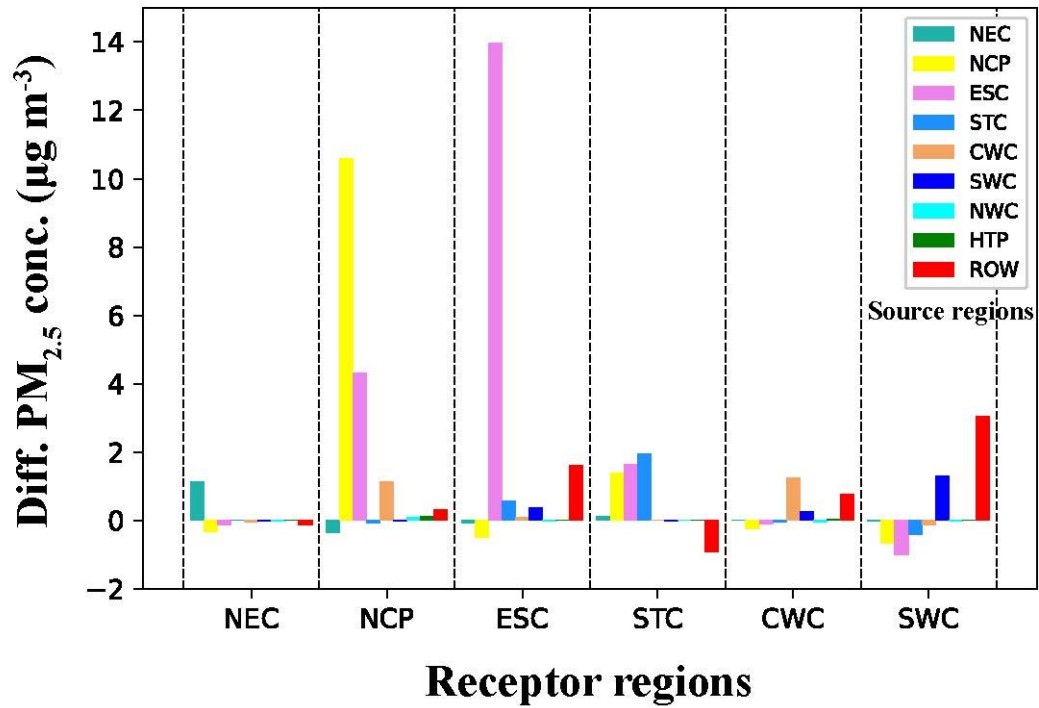
876 **Figure 76.** Relative contributions (%) of (a) local emissions, (b) the emissions from the  
877 rest of China (RCN) and (c) all sources outside China (rest of the world, ROW) to  $PM_{2.5}$   
878 column burden during the three time periods.

879



880  
881  
882  
883  
884  
885  
886

**Figure 87.** Composite differences in winds at 850 hPa ( $\text{m s}^{-1}$ ) and near-surface PM<sub>2.5</sub> concentrations ( $\mu\text{g m}^{-3}$ ) between the most polluted and normal days in February 2020. The most polluted day is defined as the day with the highest daily PM<sub>2.5</sub> concentration in February 2020 in each receptor region in China.



887

888

889 **Figure 98.** Composite differences in near-surface PM<sub>2.5</sub> concentrations (µg m<sup>-3</sup>)  
 890 averaged over receptor regions (marked on the horizontal axis) in China between [the](#)  
 891 [most](#) polluted and normal days in February 2020 originating from individual source  
 892 regions (corresponding color bars in each column).